

# Partitioning carbon sources between wetland and well-drained ecosystems to a tropical first-order stream - Implications to carbon cycling in the whole watershed (Nyong, Cameroon)

Moussa Moustapha<sup>1</sup>, Loris Deirmendjian<sup>2, 3</sup>, David Sebag<sup>4, 5, 6</sup>, Jean-Jacques Braun<sup>2, 3, 7, 8</sup>, Stéphane Audry<sup>2</sup>, Henriette Ateba Bessa<sup>7</sup>, Thierry Adatte<sup>9</sup>, Carole Causserand<sup>2</sup>, Ibrahima Adamou<sup>1</sup>, Benjamin Ngounou Ngatcha<sup>1</sup>, Frédéric Guérin<sup>2, 3</sup>.

<sup>1</sup>Université de Ngaoundéré, Faculté des Sciences, BP 454 Ngaoundéré, Cameroun

<sup>2</sup>Géosciences Environnement Toulouse (GET-Université de Toulouse, CNRS, IRD), Université de Toulouse Paul Sabatier, 14 Avenue Edouard-Belin, 31400 Toulouse, France

10 <sup>3</sup>IRD, UR 234, GET, 14 Avenue E. Belin, 31400, Toulouse, France

<sup>4</sup>Normandie Univ, UNIROUEN, UNICAEN, CNRS, M2C, 76000 Rouen, France

<sup>5</sup>HSM, IRD, CNRS, Université de Montpellier, Montpellier, France

<sup>6</sup>IFPEN, Geosciences Dept, Rueil-Malmaison, France

<sup>7</sup>Institut de Recherches Géologiques et Minières/Centre de Recherches Hydrologiques, BP 4110, Yaoundé, Cameroun

15 <sup>8</sup>International Joint Laboratory DYCOFAC, IRGM-UY1-IRD, Rue Joseph Essono Balla, Quartier Elig Essono, BP 1857, Yaoundé, Cameroun

<sup>9</sup>Institut des Sciences de la Terre (ISTE), Université de Lausanne, GEOPOLIS, CH-1015 Lausanne, Switzerland

Correspondence to: Frédéric Guérin ([frederic.guerin@ird.fr](mailto:frederic.guerin@ird.fr))

## Abstract

20 Tropical rivers emit large amounts of CO<sub>2</sub> to the atmosphere, in particular due to great wetland to river carbon (C) inputs. Yet, tropical African rivers remain largely understudied and little is known about the partitioning of C sources between wetland and well-drained ecosystems to rivers. In the Nyong watershed (Cameroon, 27 800 km<sup>2</sup>), we fortnightly measured in groundwater located in a well-drained forest (hereafter referred as non-flooded forest groundwater) and in stream orders 1 to 6, total alkalinity, dissolved inorganic C (DIC) used together with pH to compute the partial pressure of CO<sub>2</sub> (pCO<sub>2</sub>), dissolved and particulate organic C (DOC and POC) and total suspended matter. In addition, we occasionally measured heterotrophic respiration in the river. In the first-order stream, DOC and POC concentrations increased during rainy seasons when the hydrological connectivity with the riparian wetland increased whereas the concentrations of the same parameters decreased during dry seasons when the wetland was shrinking. In stream orders higher than 1, the same seasonality was observed showing that wetland in headwaters were significant sources of organic C for these rivers, even though higher POC concentration evidenced an additional source of POC in these rivers during rainy seasons that was most likely POC originating from floating macrophytes. This seasonal flush of organic matter from the wetland in the first order catchment and from the macrophytes in higher-order rivers during rainy seasons significantly affected downstream metabolism, as evidenced by lower oxygen saturation together with higher pCO<sub>2</sub> in stream orders 5 and 6 compared to 1. In the first-order catchment, the hydrological

25  
30

export of C from non-flooded forest groundwater ( $6.3 \pm 3.0 \text{ tC yr}^{-1}$ ) and wetland ( $4.0 \pm 1.5 \text{ tC yr}^{-1}$ ) to the stream represented 3-5% of the local catchment net C sink. In the first-order catchment, non-flooded forest groundwater exports 1.6 times more C than wetland, however, when weighed by surface area, C inputs from non-flooded forest groundwater and wetland to the stream contributed to 27% ( $13.1 \pm 6.2 \text{ tC yr}^{-1}$ ) and 73% ( $33.3 \pm 12.5 \text{ tC yr}^{-1}$ ) of the total hydrological C inputs, respectively. At the scale of the Nyong watershed, the yearly integrated  $\text{CO}_2$  degassing from the entire river network was  $650 \pm 160 \text{ 10}^3 \text{ tC-CO}_2 \text{ yr}^{-1}$  ( $23.5 \pm 5.6 \text{ tC km}^{-2} \text{ yr}^{-1}$ ) whereas average heterotrophic respiration in the river and  $\text{CO}_2$  degassing rates were  $99 \pm 27$  and  $1160 \pm 580 \text{ mmol m}^{-2} \text{ d}^{-1}$ , which implied that only  $\sim 8.5\%$  of the degassing at the water-air interface was supported by heterotrophic respiration in the river. In addition, the total fluvial C export of  $190 \pm 100 \text{ 10}^3 \text{ tC yr}^{-1}$  ( $10.3 \pm 5.9 \text{ tC km}^{-2} \text{ yr}^{-1}$ ) plus the yearly integrated  $\text{CO}_2$  degassing from the entire river network represented  $\sim 10\%$  of the net C sink estimated for the whole Nyong watershed. Finally, we highlight that attributing to a unique terrestrial source the whole amount of riverine C emitted to the atmosphere and hydrologically exported at the outlet and ignoring the river–wetland connectivity might lead to the misrepresentation of C dynamics in headwaters, and thereby in the whole watershed.

## 1. Introduction

Despite their small surface area worldwide, inland waters (rivers, lakes and reservoirs) have a critical role in the global carbon (C) cycle as they receive large amount of C from the drainage of land (*terra firme* as non-flooded soils via groundwater and overland flow) and wetland (flooded soils), which is processed and subsequently transferred to the atmosphere and the ocean (Abril and Borges, 2019; Allen and Pavelsky, 2018; Cole et al., 2007; Ludwig et al., 1996; Meybeck, 1982). Besides, inland waters are significant hotspots of C dioxide ( $\text{CO}_2$ ) degassing (e.g., Raymond et al., 2013) as they are usually supersaturated with  $\text{CO}_2$  compared to the overlying atmosphere. Since the seminal paper by Cole et al. (2007) who estimated that  $0.75 \text{ PgC-CO}_2$  was emitted annually to the atmosphere from global inland waters, global emissions estimates have increased substantially. In the most spatially explicit scaling study, degassing estimate from global inland waters was  $2.1 \text{ PgC-CO}_2 \text{ yr}^{-1}$  of  $\text{CO}_2$  (Raymond et al., 2013). Later, this estimate has been updated with more accurate  $\text{CO}_2$  emissions estimates from African and Amazonian rivers and from small ponds, resulting in the latest estimate of  $3.9 \text{ PgC-CO}_2 \text{ yr}^{-1}$  to which  $0.2\text{--}0.55 \text{ PgC-CO}_2 \text{ yr}^{-1}$  might be still added as  $\text{CO}_2$  emissions estimates for rivers are usually not integrated over a full day (Borges et al., 2015a; Drake et al., 2018; Gómez-Gener et al., 2021; Holgersson and Raymond, 2016; Raymond et al., 2013; Sawakuchi et al., 2017). Globally, the latest estimate of the degassing of  $\text{CO}_2$  from inland waters was in the same order of magnitude as the net terrestrial C sink ( $3.4 \text{ PgC yr}^{-1}$ ; Friedlingstein et al., 2020).

Raymond et al. (2013) showed that  $\text{CO}_2$  emissions from global rivers ( $1.8 \text{ PgC yr}^{-1}$ ) mainly depends on emissions in tropical rivers, since these account for  $\sim 80\%$  of the global emissions. However, the magnitude of  $\text{CO}_2$  emissions from tropical rivers was poorly constrained because its estimation was based on very few data from the tropics and probably biased by the overwhelming dominance of data from the Amazon basin over other tropical basins, resulting in uncertain interpolation and

scaling. Indeed, based on CO<sub>2</sub> emissions measurements in African and Amazonian rivers including the Amazon and the Congo, Borges et al. (2015a) estimated that tropical rivers could emit alone  $1.8 \pm 0.4 \text{ PgC-CO}_2 \text{ yr}^{-1}$ . This significant flux at the global scale, estimated from direct measurements, demonstrates the importance of C emissions from tropical rivers, calling for attention to tropical systems, in particular to Africa, where very few data on C stock and C cycle are available. These data are  
70 crucial to refine the global CO<sub>2</sub> budget since tropical rivers have been identified in global earth modelling approaches as systems exhibiting higher CO<sub>2</sub> emission rates per unit area than those in the temperate and boreal regions (Lauerwald et al., 2015; Raymond et al., 2013). In addition, in these modelling studies the CO<sub>2</sub> emission upscaling was done using the GLORICH dataset, in which the water CO<sub>2</sub> partial pressure (pCO<sub>2</sub>) is actually estimated from pH and total alkalinity (TA). This calculation method leads to overestimate pCO<sub>2</sub> up to 75 times, notably in low buffered and high organic waters, which are representative  
75 for boreal and tropical rivers (Abril et al., 2015).

The dissolved CO<sub>2</sub> in riverine waters originates concomitantly from heterotrophic respiration in the river, i.e., from the decomposition of organic matter (OM) in the aquatic system itself, and from the drainage of land and wetland (Abril and Borges, 2019; Borges et al., 2015; Hotchkiss et al., 2015). In tropical watersheds, riverine respiration is usually a small  
80 component of the riverine CO<sub>2</sub> budget because of the large dominance of the drainage of land and wetland in the overall budget (e.g., Borges et al., 2019). The quantification of hydrological C fluxes originating from the drainage of land and wetland is thus fundamental to close the riverine C budget in tropical watersheds. In the Amazon and the Congo watersheds, the intensity of the CO<sub>2</sub> degassing from the rivers has been related to the percentage of the wetland cover (Abril et al., 2014; Borges et al., 2019, 2015b), showing that wetlands are the main source of OM fuelling CO<sub>2</sub> production in tropical watersheds. Indeed,  
85 tropical wetlands are productivity hotspots and a large fraction of their biomass is released to the water through litter-fall and roots exudation, which fuels heterotrophic respiration in the wetland and enrich the water in CO<sub>2</sub> (Abril et al., 2014; Abril and Borges, 2019). The drainage of wetlands also releases large amounts of OM directly to the rivers, enhancing heterotrophic respiration in the river and therefore supports CO<sub>2</sub> degassing from the rivers (Abril et al., 2014; Abril and Borges, 2019). Still, in tropical watersheds, questions remain about the quantification and partitioning of hydrological C fluxes originating from  
90 the drainage of land and wetland at the plot scale and their significance in comparison to the local net terrestrial C sink (Duvert et al., 2020a). At smaller scale, the very few studies that compare the local net terrestrial C sink with direct measurements of the hydrologic export of C from land showed that only a small fraction (between 3 and 7%) of the net terrestrial C sink is actually exported to the aquatic environment, whether in temperate or tropical ecosystems (Deirmendjian et al., 2018; Duvert et al., 2020a; Kindler et al., 2011), but to the best of our knowledge this kind of work has never been done in tropical Africa.  
95 As the hotter and wetter conditions expected in tropical Africa in a near future will likely modify C fluxes at the watershed scale, integrative studies on C cycling in tropical watersheds are required to understand the present conditions and thus to better predict future changes (Duvert et al., 2020a).

The Nyong River basin (South Cameroon) belongs to the Critical Zone Observatories' (CZOs; Gaillardet et al., 2018) network named Multiscale TROPical CatchmentS (M-TROPICS; <https://mtropics.obs-mip.fr>; Audry et al., 2021) and is a long-term monitoring program of hydrological and environmental parameters in the tropics. In this study, we used rainfall, water table level and river discharges measured in the framework of the M-TROPICS observatory. The first objective of this study is to estimate the riverine C budget of a first-order catchment, the Mengong catchment, a nested sub-catchment of the Nyong watershed. The hydrological inputs of C from the drainage of land (i.e., from groundwater located in a well-drained forest; hereafter referred as non-flooded forest groundwater) and from wetland to the stream, the heterotrophic respiration in the river, the CO<sub>2</sub> degassed to the atmosphere, and the C hydrologically exported at the stream outlet are estimated and compared with the local net terrestrial C sink, and will be discussed. In lines with recent studies in large tropical watersheds (Abril et al., 2014; Borges et al., 2015; 2019), we expect that lateral inputs of C from wetland to the stream are significant in comparison with lateral inputs of C from non-flooded forest groundwater. The second objective of this study is to evaluate the changes in organic and inorganic C concentration over the seasons in the riverine continuum, from non-flooded forest groundwater to the different stream orders (order 1 to 6). Ultimately, the variations of the C concentrations in the Nyong watershed throughout a water cycle will be compared with those observed in the Mengong sub-catchment in order to evaluate how the biogeochemical cycle of C and its resulting CO<sub>2</sub> emissions to the atmosphere in a large tropical watershed is affected by the connectivity with the wetland domain.

## 2. Materials and Methods

### 2.1. Study site

#### 2.1.1. The Nyong watershed

The Nyong watershed (27 800 km<sup>2</sup>, Cameroon) is located between 2.8 and 4.5° N and 9.5 and 13.3° E, mainly in the Southern Cameroon Plateau (600-900 m high) (Fig. 1). The landscape of the Southern Cameroon Plateau mostly consists in a succession of convex rounded hills separated by flat wetlands of variable sizes (Olivry, 1986). We adopt the common definition of wetlands as habitats with continuous, seasonal, or periodic standing water or saturated soils (Mitsch et al., 2012). The main stem (the Nyong River, stream order 6) is 690 km long and is flowing west to the Atlantic Ocean (Fig.1). In the eastern part of the watershed (from Abong Mbang to Akonolinga; Fig. 1), the Nyong River is flowing through large riparian wetlands of variable size according to seasons, up to 2-3 km width (Olivry, 1986). In the western part of the basin (downstream to Akonolinga; Fig. 1), riparian wetlands extent is less pronounced and the Nyong river is flowing through mature forest in a well-channelled river bed (Olivry, 1986).

The Nyong watershed experiences an equatorial climate with four seasons of unequal importance with two maxima and minima: a short rainy season (SRS: Apr-June), a short dry season (SDS: July-August), a long rainy season (LRS: Sept.-Nov)

130 and a long dry season (LDS: Dec-March) (Suchel, 1987). The catchment lithology is composed of metamorphic and plutonic rocks with the absence of carbonate rocks and minerals (Viers et al., 2000). Slopes and hills are recovered by a thick lateritic profile (20-40 m) poor in C, whereas in the wetlands (i.e., in the depressions) the upper part of the hydromorphic soils shows an enrichment in OM (Boeglin et al., 2003; Nyeck et al., 1999). Ferrealitic soils covers about 80% of the Nyong watershed, and this soil cover can reach 40 m thick (Braun et al., 2005). On hills and hillsides, the vegetation cover is dominated by semi  
135 deciduous-forest whereas in the wetlands *Raffia* palm trees usually dominates.

In the Nyong watershed, six sites were sampling fortnightly from January to December 2016 (22 times during the sampling period), namely from upstream to downstream: the small first-order Mengong catchment (at the source and the outlet of the catchment), the Awout River (order 3), the So'o River (order 4), and the Nyong River at Mbalmayo (order 5) and Olama (order  
140 6); all sampling sites were located in the western part of the watershed (Table 1; Fig. 1). Noteworthy, the Mengong catchment is described in detail in the next section 2.1.2. The Awout River is flowing for about 30 km in a partially marshy river bed. The So'o River is the southern forest extension of the Nyong Watershed and is the main tributary on the left bank of the Nyong River. The Mbalmayo sampling station is located on the Nyong River upstream the confluence with the So'o, while the Olama sampling station is located downstream this confluence. Each sampling site (except the Mengong source) are gauging stations  
145 calibrated for discharges measurements, monitored daily since 1998 and are publicly available at <https://doi.org/10.6096/BVET.CMR.HYDRO> (Audry et al., 2021). The yearly average discharge of the Nyong River at Olama was  $\sim 195 \text{ m}^3 \text{ s}^{-1}$  for both the 1998-2020 period (long-term average) and the year of sampling 2016. Also, the average monthly discharges during the year 2016 did not differ significantly from the average monthly discharges from the 1998-2020 period (Fig. 2). The annual rainfall in the Nyong watershed was 1986 mm in 2016 which is in the upper range of rainfall ( $1600 \pm 290$   
150 mm) for the 1998-2020 period (Fig. 2). Altogether, this shows that hydrological fluxes occurring during the sampling year 2016 were typical of the hydrological fluxes usually occurring in the Nyong watershed.

In addition, the C exported at the most downstream station (Nyong at Olama) is considered as representative as the C exported to the Atlantic Ocean by the whole Nyong watershed because the contribution of the tributaries downstream from this station  
155 is negligible (Nkoue-ndondo, 2008). Indeed, Brunet et al. (2009) measured both hydrological export of DIC and DOC from the Nyong River at Olama and also more downstream near Déhané (very close to the Nyong river outlet; Fig. 1) and they showed that these fluxes (in  $\text{tC km}^{-2} \text{ yr}^{-1}$ , weighed by the catchment surface area drained at Olama or Edea) were similar at Olama ( $4.2 \pm 0.1$  and  $0.8 \pm 0.1 \text{ tC km}^{-2} \text{ yr}^{-1}$ , for DOC and DIC, respectively) and Déhané ( $3.9 \pm 0.2$  and  $1.1 \pm 0.1 \text{ tC km}^{-2} \text{ yr}^{-1}$ ).

### 2.1.2. The first-order Mengong catchment

160 The Mengong Catchment is 0.6 km<sup>2</sup> and consists of a convexo-concave landscape, ranging from 669 m at the river outlet to 703 m at the top of the hill, separated by a flat wetland that covers 0.12 km<sup>2</sup> (Fig. 3). Semi-deciduous rainforest (*Sterculiaceae-Ulmaceae*, C3 plant) covers most of the hills and hillsides, whereas most of the wetland vegetation comprises semi-aquatic plants of the Araceae family (C4) and tree populations of *Gilbertiodendron deweveri* (*Caesalpinaceae*, C3) and *Raffia monbuttorum* (raffia palm trees, C3) (Braun et al., 2005, 2012). The hillside soil cover is a thick lateritic soil that consists of a  
165 succession of four main horizons, namely from the bottom to the top, the saprolitic horizon, the mottled clay horizon, the ferruginous horizon, and the soft clayey topsoil; the thickness and distribution of these soil layers depend on the topographic position (Fig. 3). The groundwater floods the fractured bedrock, the entire saprolite, and partly the mottled clay horizon (Braun et al. 2005; Fig. 3). The soil cover is 15 m thick at the top of the north hill (piezometer 1); the depth however, decreases progressively towards the flat wetland (Fig. 3). The roots of the hillside vegetation are essentially located in the topsoil horizon,  
170 which has a depth of 5 to 6 m at the top of the hill (at piezometer 1) and has a depth of 3 to 4 m (at piezometer 2) at the mid-slope (Braun et al. 2005; Fig. 3). In the wetland, a dark-brown organic-rich sandy material with a thickness ranging from 0.1 to 1 m tops the hydromorphic soil. In this organic horizon, OM can reach up to 20% by weight, and it is composed of a thick mat of dead and living roots and tubers originating from the wetland vegetation (Braun et al. 2005; Fig. 3). Noteworthy, the first-order Mengong catchment is considered representative of the South Cameroon plateau (and thus of the Nyong watershed)  
175 that also consists itself in multiconvex land form developed on granitic terrains separated by flat wetland (Braun et al., 2012). Moreover, the same soil cover and plant species are observed in the Mengong catchment and in the Nyong watershed but it should be noted that the wetland extent is larger in the Mengong Catchment (20%) than in the whole watershed (~5%) (Table. 1). Note that wetland extent in catchment higher than 1 were estimated from GIS analysis using the global wetland map by Gumbrecht et al., 2017).

180 Groundwater draining the hillside emerges at two sources ( $Q_{\text{hill}}$ ) in the watershed head and at specific seepage points ( $Q_{\text{base}}$ ) along the hillside/wetland boundaries (Fig. 3). Only one of these two sources is perennial, the other dries up during dry periods (Fig. 3; Braun et al., 2005; Maréchal et al., 2011). Note that groundwater that emerges at sources and at specific seepage points will be further referred as non-flooded forest groundwater.  $Q_{\text{hill}}$  is conveyed to the stream with negligible interaction with the  
185 wetland, while  $Q_{\text{base}}$  fed the wetland, which is flooded all year long (Maréchal et al., 2011). In addition, according to observations made in the Mengong catchment during most of the rainfall events by Maréchal et al. (2011), it is assumed that the overland flow can be neglected on the forested hillside as the porous soil have a high infiltration capacity. Therefore, the water budget of the hillside aquifer system, as shown in Fig. 3, is the following:

$$R_{\text{hill}} = Q_{\text{hill}} + Q_{\text{base}} \quad (\text{Eq. 1})$$

190 where,

$R_{hill}$  is the recharge rate of the hillside by infiltration of rain water. Maréchal et al. (2011) estimated  $R_{hill}$  at 20% of the yearly rainfall occurring in the Mengong catchment, based on a hydrological model related to chloride mass balance at the catchment scale.  $Q_{hill}$  and  $Q_{base}$  represents 90 and 10% of  $R_{hill}$ , respectively.

195 The total streamflow at the outlet of the Mengong catchment ( $Q_{ST}$ ), as shown in Fig. 3, is the sum of the contributions of  $Q_{hill}$ , the exchange flow between the wetland and the stream ( $Q_{WL/ST}$ ) and the overland flow on the wetland surface ( $OF_{WL}$ ), as the following:

$$Q_{ST} = Q_{hill} + Q_{WL/ST} + OF_{WL} \quad (Eq. 2)$$

where,

200  $OF_{WL}$  represents 35% of the of the yearly rainfall in the Mengong catchment (Maréchal et al. 2011). Note that both  $Q_{hill}$  and  $OF_{WL}$  can be estimated from the yearly rainfall over the Mengong catchment and  $Q_{ST}$  is measured.  $Q_{WL/ST}$  can be thus obtained by difference, but only on a yearly basis.

## 2.2. Sampling and laboratory work

The water samples in the Nyong, So'o and Awout Rivers were collected from bridges using a Niskin Bottle (3L) attached to a  
 205 rope. At the Mengong source, the water samples were taken directly from the source where non-flooded forest groundwater seeps out from a polyvinyl chloride pipe. Note that the pipe is only a few centimetres long, thus limiting considerably the contact time between water and atmospheric air. Additionally, each sampling bottle was left to overflow to avoid catching air bubble. At the Mengong outlet, the shallow depth permitted retrieving water samples directly from the stream. Dissolved inorganic C (DIC), TA, dissolved organic (DOC) and particulate organic (POC) C, total suspended matter (TSM) and the POC  
 210 content of the TSM (POC%) were measured in replicates from one-off sample. At each sampling site, we measured the physico-chemical parameters of the water (temperature, pH, oxygen saturation, and specific conductivity). In addition, we carried out 14 measurements of heterotrophic respiration in the river at two sampling sites (in the Mengong stream and in the Nyong River at Mbalmayo).

215 The water temperature, pH, oxygen saturation and specific conductivity were measured *in-situ* using portable probes (WTW®) between January and March 2016 and using an YSI® ProDSS Multiparameter Digital Water Quality Meter between April and December 2016. Calibration of sensors was carried out prior to sampling campaigns and regularly checked during the campaigns. For the WTW® probes, the conductivity cell was calibrated with a  $1000 \mu S cm^{-1}$  (25°C) standard and the pH probe was calibrated using NBS buffer solutions (4 and 7). The YSI® ProDSS was calibrated using the protocols recommended by  
 220 the manufacturer. The conditioning of water samples was done directly after the field trips in Cameroon at the Institut de Recherches Géologiques et Minières (IRGM) of Yaounde, while chemical analyses were done in France at Toulouse in the laboratory of Géosciences Et Environnement (GET). For TSM, POC and POC%, a filtration (0.5-1.5 L) was carried out on

pre-weighed and pre-combusted GF/F glass fiber filters (porosity of 0.7  $\mu\text{m}$ ). The filters were then dried at 60 °C and stored in the dark at room temperature for subsequent analysis. TSM was determined by gravimetry with a Sartorius scale (precision of the scale was  $\pm 0.1$  mg). The filters were acidified in crucibles with 2N HCl to remove carbonates and were then dried at 60 °C to remove inorganic C and the remaining acid and water and then analysed by the Rock Eval pyrolysis method to measure POC and POC% (Lafargue et al., 1998). For DOC, a portion of the POC filtrate was kept in glass bottles (60 mL) pyrolyzed beforehand, in which 3 drops of phosphoric acid (85%  $\text{H}_3\text{PO}_4$ ) were added to convert all DIC species to  $\text{CO}_2$ . The glass bottles were sealed with septa made of polytetrafluoroethylene (PTFE). DOC samples were stored at 3-5°C and DOC concentrations were measured by thermal oxidation after a DIC removal step with a SHIMADZU TOC 500 analyser in TOC-IC mode (Sharp, 1993).

We stored TA samples at 20°C in polypropylene bottles after filtration using a syringe equipped with acetate cellulose filters (porosity of 0.22  $\mu\text{m}$ ). TA was then analysed by automated electro-titration (Titrino Metrohm®) on 50 mL-samples with 0.1 N HCl as the titrant. The equivalence point was determined from pH between 4 and 3 with the Gran method (Gran, 1952). DIC samples were collected in 70 mL glass serum bottles sealed with a butyl stopper and treated with 0.3 mL of  $\text{HgCl}_2$  at 20 g  $\text{L}^{-1}$  to avoid microbial respiration during storage. Vials were carefully sealed such that no air remained in contact with samples and were stored in the dark to prevent photo-oxidation. DIC was measured with the headspace technique. The headspace was created with 15 mL of  $\text{N}_2$  gas, and 100  $\mu\text{L}$  of 85%  $\text{H}_3\text{PO}_4$  was added in the serum bottles to convert all DIC species to  $\text{CO}_2$ . After strong shaking and overnight equilibration at constant room temperature, a subsample of the headspace (1 mL) was injected with a gastight syringe into a gas chromatograph equipped with a flame ionization detector (SRI 8610C GC-FID). The gas chromatograph was calibrated with  $\text{CO}_2$  standards of 400, 1000 and 3000 ppm (Air Liquide® France). In addition, we estimated the water  $\text{pCO}_2$  from the  $\text{CO}_2\text{SYS}$  software (Lewis and Wallace Upton, 1998), using DIC, pH, water temperature measurements, and the carbonic acid dissociation constants of Millero (1979) and the  $\text{CO}_2$  solubility from Weiss (1974).

In the Mengong stream and in the Nyong River at Mbalmayo, six 70-mL serum bottles collected similarly as for DIC samples, were used for the determination of heterotrophic respiration in the river. Three serum bottles were directly poisoned in the field with 0.3 mL of  $\text{HgCl}_2$ . The three other serum bottles were incubated in a cool-dark box during 24 hours. The cool-dark box was protected from light and filled with water from the river to maintain inside the cool-dark box a water temperature similar to the one observed in the river. At the end of the incubations, the serum bottles were poisoned with 0.3 mL of  $\text{HgCl}_2$  and stored in the dark and at room temperature. To estimate heterotrophic respiration in the river, we measured the increase in  $\text{CO}_2$  in the incubated serum bottles compared to those poisoned directly in the field.  $\text{CO}_2$  was measured similarly as for DIC, using the headspace technique but without a prior acidification with  $\text{H}_3\text{PO}_4$ . Noteworthy, our method does not represent total heterotrophic respiration in the river since it does not include benthic respiration. A mean benthic respiration measured in



255 various tropical rivers of  $21 \text{ mmol m}^{-2} \text{ d}^{-1}$  by Cardoso et al. (2014) will be therefore added to estimate total heterotrophic respiration in the river.

### 2.3. Determination of catchments surface area, water surface area, slope and gas transfer velocity ( $k_{600}$ )

The sub-catchments surface areas and the determination of the different stream orders were estimated from the hydrological modelling tools available in QGIS3.16® and the digital elevation model (DEM, 15 sec resolution) conditioned for hydrology (HydroSHEDS; Lehner et al., 2008). In the Nyong watershed, the HydroSHEDS flowline dataset (15 sec resolution) enabled the precise determination of the total length of each stream order (1 to 6). To estimate the average monthly river width (W) in each stream order of the Nyong watershed, we used the average monthly discharges from the five gauging stations (located on stream-orders 1, 3, 4, 5 and 6) and the hydraulic equation described by Raymond et al. (2012), as follows:

$$W = 12.88Q_{\text{monthly}}^{0.42} \quad (\text{Eq. 3})$$

265 where,

$Q_{\text{monthly}}$  is the average monthly discharge in 2016 in the stream orders 1, 3, 4, 5 or 6.

Since we did not measure discharge in stream order 2, the average width of stream order 2 was extrapolated from the best exponential regression curve from the relationship between stream order and average monthly river width, as indeed, river width within a basin scale exponentially with stream order for all river orders (Strahler, 1957). We used the average monthly river width and the total length per stream order to estimate the monthly water surface area per stream order. We fused the HydroSHEDS DEM and flowline dataset to assign an altitude to each river point and thus to determine the average slope (S) per stream order. To calculate the average monthly flow velocity (V) per stream order, we used the following hydraulic equation described by Raymond et al. (2012), as follows:

$$V = 0.19Q_{\text{monthly}}^{0.29} \quad (\text{Eq. 4})$$

275 The average monthly flow velocity in stream order 2 was extrapolated from the best exponential regression curve from the relationship between stream order and monthly average flow velocity. In each stream order, the monthly gas transfer velocity normalized to a Schmidt number of 600 ( $k_{600}$  in  $\text{m d}^{-1}$ ) was derived from the parameterization as a function of S (unitless) and V ( $\text{m s}^{-1}$ ) as in the Eq. 5 by Raymond et al. (2012):

$$k_{600} = VS*2841+2.02 \quad (\text{Eq. 5})$$

280 As described by Borges et al. (2019), we chose this parameterization because it is based on the most comprehensive compilation of k values in streams which, in addition, was used in the global upscaling of CO<sub>2</sub> emissions from rivers by both Raymond et al. (2013) and Lauerwald et al. (2015).

### 2.4. C fluxes estimation at the Nyong watershed scale

#### 2.4.1. C degassing

285 In each stream order, monthly rate of CO<sub>2</sub> degassing at the water-air interface ( $F_{\text{degas}}$ ; in  $\text{mmol m}^{-2} \text{ d}^{-1}$ ) was estimated as follows:

$$F_{\text{degas}} = k_{600} K_0 (p_{\text{CO}_2\text{w}} - p_{\text{CO}_2\text{a}}) \quad (\text{Eq. 6})$$

where,

$K_0$  is the solubility coefficient of  $\text{CO}_2$  determined from the water temperature (Weiss, 1974),  $k_{600}$  is the monthly gas transfer velocity of  $\text{CO}_2$  (section 2.3),  $p_{\text{CO}_2\text{w}}$  and  $p_{\text{CO}_2\text{a}}$  are the monthly partial pressures of  $\text{CO}_2$  in the surface waters of the different stream orders and in the overlying atmosphere (set to 400 ppmv), respectively.

In each stream order, we multiplied monthly  $F_{\text{degas}}$  in  $\text{mmol m}^{-2} \text{d}^{-1}$  by the respective monthly water surface area to estimate the monthly  $\text{CO}_2$  emissions ( $F_{\text{degas}}$  in  $\text{tC yr}^{-1}$ ) integrated in each stream order. We summed  $F_{\text{degas}}$  in  $\text{tC yr}^{-1}$  in each stream order to estimate the total quantity of  $\text{CO}_2$  degassed from the Nyong watershed from the entire river network and then normalized by the Nyong watershed area ( $\text{tC km}^{-2} \text{yr}^{-1}$ ). Note, we did not measure  $p_{\text{CO}_2}$  in second-order streams but estimated the  $p_{\text{CO}_2}$  by averaging the  $p_{\text{CO}_2}$  measured in the first- and third-order streams.

#### 2.4.2. C export to the ocean

The C hydrologically exported to the ocean ( $F_{\text{ocean}}$ ) was calculated monthly at the most downstream station (Nyong at Olama) as the following:

$$F_{\text{ocean}} = Q_{\text{olama}} [C]_{\text{olama}} \quad (\text{Eq. 7})$$

where  $Q_{\text{olama}}$  and  $[C]_{\text{olama}}$  are the monthly average discharges and concentrations of POC, DIC or DOC at Olama, respectively.  $F_{\text{ocean}}$  was estimated in  $\text{tC yr}^{-1}$  and then normalized by the catchment surface area at Olama ( $\text{tC km}^{-2} \text{yr}^{-1}$ ).

### 2.5. Riverine C budget of the first-order Mengong catchment

#### 2.5.1. The different C fluxes

At the Mengong catchment scale, as described above in the section 2.1.2, there are two sources fuelling the Mengong stream with C, namely non-flooded forest groundwater ( $F_{\text{GW}}$ ) and wetland ( $F_{\text{WL}}$ ). The C entering the Mengong stream has two outputs as this C is either degassed at the water-air interface ( $F_{\text{D}}$ ) or hydrologically exported at the stream outlet ( $F_{\text{OUT}}$ ). Noteworthy, heterotrophic respiration in the stream ( $F_{\text{RH}}$ ) is considered as an C input for the DIC budget, while a C output for the DOC budget (assuming respiration occurs on DOC only). Riverine DIC, DOC and POC budgets ( $\text{DIC}_{\text{budget}}$ ,  $\text{DOC}_{\text{budget}}$ ,  $\text{POC}_{\text{budget}}$ ) are thus the difference between C inputs and outputs as follows:

$$\text{DIC}_{\text{budget}} = F_{\text{GW}} + F_{\text{WL}} + F_{\text{RH}} - F_{\text{D}} - F_{\text{OUT}} \quad (\text{Eq. 8})$$

$$\text{DOC}_{\text{budget}} = F_{\text{GW}} + F_{\text{WL}} - F_{\text{RH}} - F_{\text{OUT}} \quad (\text{Eq. 9})$$

$$\text{POC}_{\text{budget}} = F_{\text{WL}} - F_{\text{OUT}} \quad (\text{Eq. 10})$$

Noteworthy, these C budgets at the Mengong catchment scale cannot be estimated monthly as for  $F_{\text{degas}}$  or  $F_{\text{ocean}}$  at the Nyong watershed scale, because water fluxes described in Equations 1 and 2, in particular  $Q_{\text{hill}}$  and  $OF_{\text{WL}}$ , which are needed to estimate

$F_{GW}$  and  $F_{WL}$  (see section 2.5.2), can only be estimated yearly from yearly rainfall in the Mengong catchment (see section 2.1.2).

### 2.5.2. Hydrological C inputs from non-flooded forest groundwater and wetland

According to equations 1 and 2 we can estimate the quantity of dissolved carbon leached from non-flooded forest groundwater to the Mengong stream ( $F_{GW}$ ) as the following:

$$F_{GW} = Q_{hill} [C]_{GW} \quad (Eq. 11)$$

where,

$[C]_{GW}$  is the yearly average concentration of DIC or DOC in the Mengong source.  $F_{GW}$  ( $tC\ yr^{-1}$ ) is normalized by the surface area of  $0.48\ km^2$  drained by the hillside ( $tC\ km^{-2}\ yr^{-1}$ ). Noteworthy, a part of non-flooded forest groundwater fed the wetland ( $F_{GW-bis}$ ) and can be estimated as the following:

$$F_{GW-bis} = Q_{base} [C]_{GW} \quad (Eq. 12)$$

$F_{GW-bis}$  does not account to the stream C budget because  $Q_{base}$  is not feeding the stream, but does account to the total quantity of C hydrologically leached from land.

According to equations 1 and 2, we can estimate the quantity of dissolved C leached from the wetland to the Mengong stream ( $F_{WL}$ ) as the following:

$$F_{WL} = (OF_{WL} + Q_{WL/ST}) * [C]_{WL} \quad (Eq. 13)$$

where,

$[C]_{WL}$  are the concentrations of DOC or DIC in the topsoil solution (0.4 m) of the Mengong wetland, measured at  $1\ 420 \pm 750$  and  $1\ 430 \pm 900\ \mu mol\ L^{-1}$  by Braun et al. (2005) and Nkoue Ndondo et al. (2020), respectively.  $F_{WL}$  ( $tC\ yr^{-1}$ ) is normalized by the surface area of  $0.12\ km^2$  drained by the wetland ( $tC\ km^{-2}\ yr^{-1}$ ).

In the Mengong catchment, as described in the section 2.1.2, overland flow on hillsides is negligible and there is no particulate C in non-flooded forest groundwater. Therefore, it can be safely assumed that POC at the Mengong outlet should originates mostly from the drainage and erosion of the wetland. Accordingly, it was assumed that the hydrological export of POC at the Mengong outlet is similar to the POC hydrologically exported from the wetland ( $F_{WL}$ ). For POC,  $F_{WL}$  can thus be estimated as the following:

$$F_{WL} = Q_{outlet} [POC]_{OUT} \quad (Eq. 14)$$

where,

$Q_{outlet}$  and  $[POC]_{OUT}$  are the yearly average discharge and POC concentration at the Mengong outlet, respectively.  $F_{WL}$  ( $tC\ yr^{-1}$ ) is normalized by the surface area of the wetland ( $tC\ km^{-2}\ yr^{-1}$ ).

### 2.5.3. C degassing

It has been shown that a large fraction of C degassing in headwaters was actually missed by conventional stream sampling because a large fraction of the degassing occurs as hotspots in the vicinity of groundwater resurgences (e.g., Deirmendjian and Abril, 2018; Johnson et al., 2008). Therefore, we estimated  $F_D$  from a mass balance that calculates the loss of the dissolved  $CO_2$  between non-flooded forest groundwater ( $F_{D-GW}$ ) (or wetland;  $F_{D-WL}$ ) and stream water, using  $CO_2$  concentrations and drainage data, a method similar to Duvert et al. (2020a), as the following

$$F_{D-GW} = ([CO_2]_{GW} - [CO_2]_{OUT}) * Q_{Hill} \quad (Eq. 15)$$

$$F_{D-WL} = ([CO_2]_{WL} - [CO_2]_{OUT}) * (OF_{WL} + Q_{WL/ST}) \quad (Eq. 16)$$

$$F_D = F_{D-GW} + F_{D-WL} \quad (Eq. 17)$$

where,

$[CO_2]_{GW}$ ,  $[CO_2]_{WL}$  and  $[CO_2]_{OUT}$  are the yearly average  $CO_2$  concentrations in non-flooded forest groundwater, wetland, and stream outlet, respectively.

### 2.5.4. C hydrologically exported at the Mengong stream outlet

Based on equation 3, the quantity of C hydrologically exported at the outlet of the Mengong catchment can be estimated as the following:

$$F_{OUT} = Q_{ST} [C]_{OUT} \quad (Eq. 18)$$

where,  $[C]_{OUT}$  is the concentration of POC, DOC or DIC at the Mengong stream outlet, respectively.

### 2.5.5. Heterotrophic respiration in the stream

$F_{RH}$  in  $mmol\ m^{-3}\ d^{-1}$  is the average heterotrophic respiration in the Mengong stream obtained from the increase in  $CO_2$  in the incubated serum bottles over 24h.  $F_{RH}$  was converted in  $mmol\ m^{-2}\ d^{-1}$  by multiplying by the average depth at the Mengong stream outlet.

## 3. Results

### 3.1. Hydrology

In 2016, the discharges were  $0.009 \pm 0.002$  (range was 0-0.35),  $3.9 \pm 4.8$  (0-35),  $35.6 \pm 40.6$  (3.4-175),  $146 \pm 112$  (21-392) and  $195 \pm 160$  (8-640)  $m^3\ s^{-1}$ , in stream orders, 1, 3, 4, 5 and 6, respectively (Table 1, Fig. 2). All river discharges seasonally peaked twice a year during the two rainy seasons, both separated by dry seasons; the groundwater water table followed the same trend (Figs. 2, 4-5). Specifically, the beginning to middle of the rainy seasons corresponded to a period of increasing river discharge and groundwater water table level, while the end of the rainy seasons and the dry seasons corresponded to a period of decreasing river discharge and groundwater water table level (Figs. 2, 4-5). In each stream order, low-water period and lowest discharges

were observed during the long dry season (Figs. 2). The stream orders 1 and 3 were dried up during the long dry seasons (from the 01<sup>st</sup> Jan. to the 15<sup>th</sup> Mar. 2016 and to the 28<sup>th</sup> Apr. 2016, for stream order 1 and 3, respectively) whereas the streams with orders higher than 3 were never dried up (Fig. 2).

### 3.2. Seasonal variations of C and ancillary parameters in non-flooded forest groundwater

380 Yearly averages and ranges in C and ancillary parameters in non-flooded forest groundwater are detailed in Tables 2 and 3. The coefficients of variation of groundwater temperature, pH and specific conductivity were lower than 5% showing a strong stability for these parameters throughout the water cycle. Oxygen saturation in non-flooded forest groundwater increased during the long dry season and peaked at the end of the same season (up to 68% the 30<sup>th</sup> Mar. 2016), then slowly decreased towards the end of the long rainy season (down to 38% the 15<sup>th</sup> Nov. 2016) (Fig. 4). pCO<sub>2</sub> in non-flooded forest groundwater  
385 concentration exhibited strong temporal variations (coefficient of variation was about 50%), and peaked in the middle of the short (up to 100 000 ppmv the 16<sup>th</sup> Feb. 2016) and long (up to 200 000 ppmv the 01<sup>st</sup> Aug. 2016) dry seasons, while decreasing during the two wet seasons (Fig. 4). All year long, DOC in non-flooded forest groundwater was below the detection limit of 1 mg L<sup>-1</sup> (<83 µmol L<sup>-1</sup>); note we considered this threshold as the average DOC concentration in non-flooded forest groundwater. Despite one peak of TA that was up to 138 µmol L<sup>-1</sup> the 29<sup>th</sup> Sep. 2016, TA in non-flooded forest groundwater was relatively  
390 stable through the water cycle (Fig. 4).

### 3.3. Seasonal variations of C and ancillary parameters in surface waters

Yearly averages and ranges in C and ancillary parameters in surface waters are detailed in Tables 2 and 3. In streams orders 1 and 3 variations of pH, specific conductivity and oxygen saturation were weakly affected by the discharge as indicated by non-correlations between these parameters and the discharge in these streams (Table 4, Fig. 5). Nonetheless, in the stream order 3,  
395 we observed an increased in oxygen saturation during dry periods (Fig. 5). On the contrary, in streams orders 4, 5 and 6, variations of pH, specific conductivity and oxygen saturation as a function of river discharge were more pronounced as these parameters peaked during dry seasons and decreased during rainy seasons as indicated by significant negative correlations between these parameters and the discharge in these streams (Table 4, Fig. 5).

400 DOC concentration in stream order 1 increased at the beginning of the re-flowing period (i.e., at the beginning of the short rainy season, up to 4 140 µmol L<sup>-1</sup> the 14<sup>th</sup> Apr. 2016) (Fig. 5). In the other stream orders, a similar DOC trend occurred but with a slight delay of about a couple of weeks in comparison to the one observed in stream order 1 (Fig. 5). After this seasonal peak, DOC concentration quickly decreased to reach minimum values during the following short dry season, then DOC concentration was rather stable until the first rains fall again in the next short rainy season (Fig. 5). In stream order 1, POC and  
405 TSM concentrations also peaked significantly at the beginning of the re-flowing period, driving the negative correlation of these two parameters with the discharge in this stream; we did not observe a similar increase in higher order streams (Table 4; Fig. 5). In addition, in stream order 1, POC%, POC and TSM concentrations increased during the two wet seasons, while

decreased during the short dry season; a similar trend was observed in stream orders 5 and 6 as indicated by the positive correlation between POC and TSM and the discharge in these streams (Table 4; Fig. 5). In contrast, in stream orders 3 and 4, TSM concentration did not follow this trend as it peaked during short dry season and at the beginning of the long dry season (Fig. 5).

In all stream orders, we observed an increase in TA concentration during the long rainy season followed by a quick decrease (Fig. 5). Overall, there was also a peak in TA concentration at the end of the long dry season followed by a decrease during the following short rainy and dry seasons, driving the significant negative correlation between discharge and TA concentration in stream orders 4, 5 and 6 (Table 4, Fig. 5). In the stream order 1,  $pCO_2$  exhibited a similar trend to the POC, with values peaking during the two wet seasons (Fig. 5). In stream orders higher than 1,  $pCO_2$  seasonally peaked during the long rainy season, but more significantly in stream orders 5 and 6 as indicated by the positive correlation between  $pCO_2$  and discharge in these streams (Table 4).

### 3.4. Spatial variations of C and ancillary parameters across non-flooded forest groundwater, and increasing stream orders

TSM and POC concentrations were not significantly different in streams orders 3, 5 and 6, but were significantly lower in stream order 1, while being significantly higher in stream order 4 ( $p<0.001$ , Kruskal-Wallis with Dunn's multiple comparisons tests) (Fig. 6). POC content of the TSM was significantly higher in stream order 1 in comparison to all other stream orders, while not being significantly different between stream orders 3 to 6 ( $p<0.05$ , Kruskal-Wallis with Dunn's multiple comparisons tests) (Fig. 6). DOC concentration was not significantly different between streams orders 1, 4, 5 and 6, but was significantly lower in non-flooded forest groundwater, while being significantly higher in stream order 3 ( $p<0.001$ , Kruskal-Wallis with Dunn's multiple comparisons tests) (Fig. 6).

The oxygen saturation was not significantly different between non-flooded forest groundwater and streams orders 1, 3 and 4, whereas it was significantly lower in the Nyong River (streams orders 5 and 6) ( $p<0.05$ , Kruskal-Wallis with Dunn's multiple comparisons tests) (Fig. 6). TA concentration was significantly higher in stream order 1 than in non-flooded forest groundwater ( $p>0.01$ , Mann-whitney test) (Fig. 6) (Fig. 5). In addition, TA concentration was significantly higher in streams orders 5 and 6 than in non-flooded forest groundwater and in streams orders 1, 3 and 4 ( $p<0.001$ , Kruskal-Wallis with Dunn's multiple comparisons tests) (Fig. 6).  $pCO_2$  was significantly higher in non-flooded forest groundwater, while was similar in all other stream orders ( $p<0.001$ , Kruskal-Wallis with Dunn's multiple comparisons tests) (Fig. 6).

### 3.5. C budget at the Mengong catchment scale

The DIC<sub>budget</sub> was well-balanced, showing inputs and outputs fluxes not statistically different ( $p>0.05$ ; Mann-Whitney test) and differing only by 6%. This indicate that all DIC fluxes have been considered and well constrained (Table 5). In contrast, the DOC<sub>budget</sub> was not balanced, showing statistically different inputs and outputs fluxes ( $p<0.001$ ; Mann-Whitney test) by 235%. This shows that unidentified DOC inputs were overlooked from the estimated budget (Table 5). The quantity of hydrologically exported C from non-flooded forest groundwater ( $F_{GW} + F_{GW-bis}$ ) was  $7.0\pm 3.0$  tC yr<sup>-1</sup> ( $14.6\pm 6.2$  tC km<sup>-2</sup> yr<sup>-1</sup>). Noteworthy, 10% of this export go to the wetland rather than the stream; and 97% of this hydrological export of C occurred as DIC (Fig. 7). The annual flux of the hydrologically exported C from wetland to the stream ( $F_{WL}$ ) was  $4.0\pm 1.6$  tC yr<sup>-1</sup> ( $33.3\pm 12.5$  tC km<sup>-2</sup> yr<sup>-1</sup>); DOC, DIC and POC contributing for 45, 45 and 5%, respectively (Fig. 7). The annual flux of C degassed to the atmosphere as CO<sub>2</sub> ( $F_D$ ) was  $5.5\pm 2.3$  tC yr<sup>-1</sup>, while the heterotrophic respiration in the stream ( $F_{RH}$ ) was  $0.3\pm 0.1$  tC-CO<sub>2</sub> yr<sup>-1</sup> (Fig. 7)

### 3.6. C degassing and C export to the ocean at the Nyong watershed scale

Spatially, yearly averages of monthly  $k_{600}$  increased from stream order 1 ( $2.2\pm 0.1$  m d<sup>-1</sup>) to 4 ( $3.0\pm 0.3$ ) and subsequently decreased downstream in stream orders 5 ( $2.3\pm 0.1$ ) and 6 ( $2.5\pm 0.2$ ). In contrast, monthly  $k_{600}$  did not exhibit much seasonal variations (Table 6; Fig. S1). Spatially, yearly averages of monthly CO<sub>2</sub> degassing rates were similar in stream orders 1, 2, 3 and 4 but significantly lower in stream orders 5 and 6 ( $p<0.001$ , Kruskal-Wallis with Dunn's multiple comparisons tests) (Table 6). Rates of heterotrophic respiration were  $46\pm 22$  and  $151\pm 31$  mmol m<sup>-2</sup> d<sup>-1</sup> in stream order 1 and 5, respectively, whereas CO<sub>2</sub> degassing rates were  $1220\pm 640$  and  $846\pm 350$  mmol m<sup>-2</sup> d<sup>-1</sup> in the same stream orders, respectively (Table 6). Seasonally, considering all stream orders, the monthly average CO<sub>2</sub> degassing rates during rainy seasons were in average 20% higher in comparison to average CO<sub>2</sub> degassing rates during dry seasons, explaining higher integrated CO<sub>2</sub> degassing during rainy seasons at the Nyong watershed scale (Fig. 8). In addition, at the Nyong watershed scale, the yearly integrated CO<sub>2</sub> degassing ( $F_{degas}$ ) was  $650\pm 160$  10<sup>3</sup> tC-CO<sub>2</sub> yr<sup>-1</sup> ( $23.5\pm 5.6$  tC km<sup>-2</sup> yr<sup>-1</sup>); and the yearly integrated hydrological C export to the ocean ( $F_{ocean}$ ) was  $12\pm 9$  10<sup>3</sup> tC yr<sup>-1</sup> ( $0.6\pm 0.5$  tC km<sup>-2</sup> yr<sup>-1</sup>) for POC,  $130\pm 90$  10<sup>3</sup> tC yr<sup>-1</sup> ( $7.2\pm 5.4$  tC km<sup>-2</sup> yr<sup>-1</sup>) for DOC, and  $46\pm 42$  10<sup>3</sup> tC yr<sup>-1</sup> ( $2.5\pm 2.3$  tC km<sup>-2</sup> yr<sup>-1</sup>) for DIC; more than 50% of these fluxes occurring during the long rainy season (Tables 6-7; Fig. 8).

## 4. Discussion

### 4.1. Non-flooded forest groundwater and wetland as C sources in a first-order catchment

The drainage of non-flooded forest groundwater (i.e., groundwater from the hillside lateritic system) and wetland (i.e., hydromorphic system) fuels the Mengong stream with organic and inorganic C (Figs. 3, 7; Boeglin et al., 2005; Viers et al.,

1997). In the hillside lateritic system, overland flow is negligible owing to limited soil erosion due to dense vegetation cover and high soil porosity facilitating rainfall infiltration (Braun et al., 2005; Maréchal et al., 2011). Consequently, hydrological export of soil C to the stream by overland flow from the hillside is considered as negligible. In contrast to the hillside lateritic system, overland flow is a possible C pathway from the hydromorphic wetland system to the stream (Fig. 3; Maréchal et al., 2011). Thus, the stream POC shall originates mostly from the overland flow over the wetland, as also suggested by similar  $\delta^{13}\text{C}$  values of total organic carbon (TOC) in the wetland soil and in the POC observed in the stream outlet (range was -28 to -31‰) of the Mengong catchment by Nkoue-Ndondo et al. (2020). The fact that POC and TSM concentrations in the Mengong stream increased during rainy seasons, when the hydrological connectivity with the surrounding wetland is enhanced, is also in a good agreement with the identification of wetland as the main (if not exclusive) source of POC and TSM. Furthermore, Nkoue-Ndondo et al. (2020) did not observe seasonal variations of the  $\delta^{13}\text{C}$ -POC signature in the Mengong stream. This suggests that the additional POC source observed at the beginning of the reflowing period also originates from the erosion of the wetland even though this hydrological period was characterized by a weaker hydrological connectivity with the wetland compared to rainy seasons. In the Mengong wetland, litter-fall measurement by Nkoue-Ndondo (2008) was  $116 \text{ t yr}^{-1}$  of wet OM with a mean C content of 22.5%, which is equivalent to  $26 \text{ tC yr}^{-1}$ , a flux 65-times higher than our conservative estimation of the POC leached from the wetland to the stream ( $0.4 \text{ tC yr}^{-1}$ , Fig. 7). This implies that most of the wetland litter-fall accumulates in the wetland soil rather than being hydrologically exported to the stream in the form of POC, in particular due to limited overland flow in the wetland due to flat topography (Maréchal et al., 2011). However, the *in-situ* degradation of this highly labile OM might contribute to the DOC and DIC fluxes from the wetland to the stream. Indeed, tropical wetlands are recognized as productivity hotspots and a large fraction of the litter-fall is degraded *in-situ* by heterotrophic respiration in the water and sediment, enriching wetland waters in DOC and DIC (Abril et al., 2014; Borges et al., 2015a).

In the Mengong catchment, waters originating from the drainage of non-flooded forest groundwater and wetland are considered as clear and coloured waters, respectively, the colour reflecting their DOC content (Boeglin et al., 2005; Viers et al., 1997). Indeed, DOC concentration was low in clear waters ( $<83 \mu\text{mol L}^{-1}$ ) whereas it was high in coloured waters ( $1420 \pm 750 \mu\text{mol L}^{-1}$ ) (Table 3; Viers et al., 1997). The DOC in the soil solution has distinct sources that are litter leaching, root and microbial exudates, rainfall (throughfall and stemflow), and decaying fine roots (Bolan et al., 2011; Kalbitz et al., 2000). Once in the soil solution, DOC is however rapidly adsorbed onto soil minerals during its percolation through the soil column due to the soil capacity for DOC stabilization (Kothawala et al., 2009; Neff and Asner, 2001) by sorption on Fe (and Al) oxides and hydroxides and clay minerals (Kaiser et al., 1996; Kothawala et al., 2009; Sauer et al., 2007). This process significantly reduces DOC mineralisation rates in soils (Hagedorn et al., 2015; Kalbitz et al., 2005; Kalbitz and Kaiser, 2008) and DOC export from soils (Shen et al., 2015). It also partly explains the decreasing gradient of DOC concentration with depth commonly observed in boreal (e.g., Moore, 2003), temperate (e.g., Deirmendjian et al., 2018) and tropical (e.g., Johnson et al., 2006) soils. DOC sorption in soils is actually strongly related to the availability of Fe (and Al) oxides and hydroxides, and clay minerals, which



are present both in the hillside lateritic and in the hydromorphic wetland soils of the Mengong catchment (Fig. 3). In the hillside lateritic system, soil DOC is probably well stabilized in the iron-rich and clay horizons preventing DOC leaching to the non-flooded forest groundwater (Braun et al., 2005, 2012). Furthermore, DOC must be desorbed from soil minerals in order to be exported to groundwater (Deirmendjian et al., 2018; Sanderman and Amundson, 2008). Studies have shown that water saturation of the topsoil generates reducing conditions in the saturated soil (Camino-Serrano et al., 2014; Fang et al., 2016) and that this process limits the retention of soil DOC and thus enhances its export to groundwater (Deirmendjian et al., 2018).

In the hillside lateritic system, the non-flooded forest groundwater table never reaches the topsoil where soil DOC is high. Therefore, DOC adsorption in these soils might be enhanced. In the hydromorphic wetland system, the groundwater saturates the topsoil all year long (Fig. 3) which might reduce DOC adsorption in this compartment. In addition, hydromorphic conditions occurring in the Mengong wetland soil favour the solubilisation of Fe (Oliva et al., 1999), which is supposed to reduce DOC sorption. Altogether, this explains the low and high DOC concentrations observed in the non-flooded groundwater and the wetland, respectively. In addition, the results showed that stream DOC increased during the first wet season only. In the Mengong catchment, Nkounde-Ndondo (2008) described the piston flow that occurs at the beginning of the short rainy season, which is caused by new infiltration of water on the hills and hillsides that pushes the older soil water downstream (e.g., Huang et al. (2019) and references therein), allowing pressure on the aquifer and thus exfiltration at the bottom of the slope (i.e., in the wetland; Fig. 3). This implies that wetland DOC is quickly flushed during the first rains and originates from the subsurface horizons of the wetland soil. Later in the season, the decrease of stream DOC is due to dilution with non-flooded forest groundwater with low DOC content. Noteworthy, our stream DOC budget was not balanced (Table 5; Fig. 7), indicating that sources contributing to the DOC content of the Mengong stream were overlooked. An additional DOC source that was quantified by Braun et al. (2005) during 4 years in the Mengong catchment is DOC in the throughfall. These authors determined that the average DOC concentration in the throughfall was  $3.6 \pm 3.5 \text{ mg L}^{-1}$ . Applying this average concentration to the rainfall in 2016 and the catchment surface area gives an additional DOC input from precipitation of  $4.3 \pm 4.3 \text{ tC yr}^{-1}$ , which allows closing the DOC budget at the Mengong catchment scale.

Non-flooded forest groundwater and wetland exhibited high DIC concentrations,  $2\,940 \pm 1485$  and  $1\,430 \pm 900 \text{ } \mu\text{mol L}^{-1}$ , respectively and, in both systems, DIC was mostly in the  $\text{CO}_2$  form (>90%) (Table 3). In the hillside system, non-flooded forest groundwater was free of DOC. This result, along with the fact that microbial activity has been shown to be limited in many aquifers by the availability of DOC (e.g., Malard and Hervant (1999) and references therein), suggest that  $\text{CO}_2$  in non-flooded forest groundwater comes from soil respiration in the overlaying non-saturated soil - rather than respiration in the groundwater itself – and then is transported downward by diffusion rather than percolation with rain water. Indeed, the thickness of the lateritic cover on hills and slopes of the Mengong catchment considerably slows the water percolation in the bedrock (Boeglin et al., 2005). In the tropics, the soil respiration rate is mostly affected by soil moisture as soil temperature

exhibits low seasonal variations (Davidson et al., 2000). Accordingly, soil respiration rates usually decrease from rainy to dry seasons in tropical ecosystems due to decreasing soil moisture (Davidson et al., 2000). Nevertheless, in the Mengong catchment, pCO<sub>2</sub> in non-flooded forest groundwater peaked during dry seasons and started to decrease later in the same season and then during the following rainy season (Fig. 4). In mature forest of Amazonia, Johnson et al. (2008) observed a similar trend in groundwater that they attributed to an increase in vegetation water uptake and roots activity in deep soils during the onset of the dry seasons, they also showed that groundwater pCO<sub>2</sub> decreased later in the season because of losses due to drainage and diffusional losses. Furthermore, during dry seasons, the diffusion of CO<sub>2</sub> in the porous soil is facilitated in tropical forest (Adachi et al., 2006), very likely favouring the downward diffusion of soil CO<sub>2</sub> and its subsequent dissolution in groundwater, as also observed in temperate forest (Deirmendjian et al., 2018). In the non-flooded forest groundwater, oxygen saturation was about 40% but increased during dry seasons whereas decreasing during rainy seasons (Fig. 4). This shows that atmospheric air can penetrate the soil atmosphere deeply, in particular during dry seasons when the diffusion in the porous soil is facilitated, and can reach the non-flooded forest groundwater. In the wetland hydromorphic system, the soil is permanently saturated which limits aerobic respiration of microbes in the soil and leading to the accumulation of OM in the soil profile. This likely explains the lower CO<sub>2</sub> concentration observed in the wetland compared to non-flooded forest groundwater (Table 3). Nonetheless, it should be noted that wetland vegetation can actively transport oxygen to the root zone via their aerenchyma (Haase and Rätsch, 2010), creating a complex oxic-anoxic interface that promotes aerobic respiration but also supplies labile OM to anaerobic degradation (and methanogenesis) fuelling CO<sub>2</sub> (and CH<sub>4</sub>) production (Piedade et al., 2010). This is in a good agreement with δ<sup>13</sup>C-DIC signatures of -16‰ measured by Nkoue Ndondo et al. (2020) in the wetland soil, which are indeed close to the C<sub>4</sub> signature of aquatic grassland found in the Mengong wetland. In addition to drainages of non-flooded forest groundwater and wetland, stream DIC can also originate from *in-situ* respiration of DOC. This process is corroborated by our results of incubations (Table 6), and by the δ<sup>13</sup>C-DIC at the Mengong stream outlet that was more depleted in <sup>13</sup>C than in non-flooded forest groundwater and wetland (Nkoue Ndondo et al., 2020), which highlights in-stream respiration from an organic <sup>13</sup>C-depleted source.

Non-flooded forest groundwater and wetland both exhibited low TA concentrations, 53±26 and 122±46 μmol L<sup>-1</sup>, respectively; nonetheless TA concentration was significantly higher in wetland (Table 3; Fig. 6). Considering the granitic lithology (i.e., absence of carbonate minerals) of the Nyong watershed, TA in non-flooded forest groundwater and wetland might originate from the weathering of silicate minerals as dissolved CO<sub>2</sub> can react with silicate minerals to produce bicarbonates (Meybeck, 1987). Applying TA concentration in non-flooded forest groundwater into Equations 11 and 12 results in a silicate weathering rate in the overlaying lateritic soil of 0.2±0.1 tC km<sup>-2</sup> yr<sup>-1</sup>, whereas applying TA concentration in wetland into Equation 13 results in a silicate weathering rate in wetland of 1.3±0.4 tC km<sup>-2</sup> yr<sup>-1</sup>. The silicate weathering rate in wetland is thus 550% higher than in the non-flooded lateritic soil. Even though these two rates remain low compared to

weathering rates in carbonated environment, they are typical of silicate weathering rates which are in the range 0.1-5.2 tC km<sup>-2</sup> yr<sup>-1</sup> as estimated from diverse worldwide basins by Amiotte Suchet et al. (2003). In non-flooded forest groundwater, the low TA concentrations and silicate weathering rates, along with, the absence of significant seasonal variations of TA, are likely related to the relatively inert mineralogy of the lateritic soil cover (Braun et al., 2005, 2012). In the Nyong watershed, these low weathering rates are in a good agreement with the low mineral dissolved load in the aquifer (Braun et al., 2002) and by the dissolved silica fluxes in rivers that were significantly lower compared to the annual rainfall (White and Blum, 1995). In addition, weathering rates in the wetland might be enhanced by the leaching of humic acids from the vegetation to the hydromorphic soils (Braun et al., 2005; Nkoue-ndondo, 2008).

#### 4.2. Influence of wetland-river connectivity at the Nyong watershed scale

The role of wetland on riverine C cycling in tropical watersheds is commonly explored using empirical relationships between wetland extent and C concentrations in the stream water of the different sub-catchments of a given watershed. Establishing such empirical relationships in the Nyong watershed is extremely challenging owing the similar wetland extent (about 5% of the surface area; Table 1) in the sub-catchments, with the exception of the first-order Mengong catchment where the wetland extent represents 20%. However, this role can be explored by comparing the seasonality of C concentrations in stream order 1 - in which the wetland dynamic as a riverine C source has been discussed in the above section - with respect to the other stream orders. Thus, for a given parameter, similar seasonality in stream order 1 and the other stream orders might suggest that C sources and processes are similar in both (sub)systems.

Similarly to what we observed in the Mengong catchment, wetlands might be also considered as the main source of POC for surface waters in the whole Nyong watershed based on (1) the low slopes in the watershed, (2) the high infiltration capacity of the soil, (3) the similar normalized export of POC from wetland to the Mengong stream order 1 and from the Nyong watershed to the ocean (Tables 5 and 7), and (4) the probable low pelagic primary production in the surface waters of the Nyong watershed, as usually observed in tropical rivers with high DOC concentrations (>1500 µmol L<sup>-1</sup>) where light attenuation caused by browning (coloured waters) strongly limits aquatic photosynthesis (Borges et al. 2019). Moreover, the seasonality of POC was similar in stream order 1 and in high-order streams, increasing during rainy seasons while decreasing during dry seasons (Fig. 5). This suggests that in high-order streams, the POC leached from wetlands from low-order catchments might acts as an important POC source. However, during rainy seasons, the higher POC concentration observed in high-order streams in comparison to the stream order 1 (Figs. 5-6) might also suggests an additional POC source in these streams during rainy seasons. In high-order streams, given that POC% increased during rainy seasons, river bed and banks erosion is not likely as this process would have exported more TSM than POC, as observed in the tropical Tana River in Kenya by Tamooch et al. (2012). As pelagic primary production is also unlikely, POC leached from wetlands riparian to high-order streams and POC leached from floating macrophytes that develops in the river bed during the dry seasons anterior to the rainy seasons are more suitable hypotheses to explain the additional POC source observed in high-order streams. Indeed, as in the Amazonian basin

(e.g., Abril et al., 2014; Engle et al., 2008; Silva et al., 2013), we observed in high-order streams the development of floating macrophytes during dry seasons. In high-order streams, the development of these floating macrophytes was accompanied by peaks of oxygen saturation during dry seasons (Table 4; Fig. 5). This last feature is in line with the high photosynthesis capacity of macrophytes that results in oxygen-enriched water during daylight (Sabater et al., 2000). According to the flood pulse concept in tropical rivers by Junk et al. (1989), floating macrophytes might be hydrologically exported during rainy seasons when the river discharge increased sufficiently. In high-order streams of the Nyong watershed, this seasonal wetland and floating macrophytes flush of OM is also supported by other evidences such as higher pCO<sub>2</sub> and POC% along with lower oxygen saturation observed in these streams. On the one hand, these features might be attributed to enhanced heterotrophic respiration in the river fuelled by export of freshly-produced and young OM (Engle et al., 2008; Mayorga et al., 2005; Tamoooh et al., 2014). Besides, OM leached from tropical wetland can be photodegraded downstream into more labile lower molecular weight compounds that in turn also enhances heterotrophic respiration in the river, as observed in the Congo River by Lambert et al. (2016). On the other hand, the drainage of wetland can also directly account for CO<sub>2</sub> emissions from surface waters as under flooded conditions, roots and microbial respiration occurring in wetland directly release CO<sub>2</sub> to the water (Abril et al., 2014; Moreira-Turcq et al., 2013). These two patterns usually explain the positive correlation between pCO<sub>2</sub> and river discharge in tropical systems (Table 4; Borges et al., 2019). On the contrary, during dry periods, the wetlands are shrinking and the river become more hydrologically disconnected from wetlands, explaining the lower pCO<sub>2</sub> in tropical rivers during dry seasons (Abril and Borges, 2019). The importance of river-wetland connectivity was also evidenced by the first POC increase at the beginning of the re-flowing period that was not observed downstream (Fig. 5). This suggests POC was quickly oxidized *in-situ*, or did not reach downstream due to weak hydrological connectivity with high-order streams during this period. Indeed, when the Mengong (stream order 1) was flowing again, the downstream Awout River (stream order 3) was still dry. This highlights the complex deposition and remobilisation cycles of TSM and POC in tropical rivers (Geeraert et al., 2017; Moreira-Turcq et al., 2013). Finally, in stream orders 3 and 4, we observed an additional increase of TSM during dry seasons, while POC% decreased (Fig. 5). This suggests that more TSM than POC was leached into these streams during dry seasons. We assume that river bed and banks erosion could drive this seasonal trend. In the tropical Tana River in Kenya, based on radionuclide's ratio reflecting the age of TSM, Tamoooh et al. (2014) showed that TSM was old and increased during dry seasons. This was attributed to inputs of older sediments, with river banks erosion and/or resuspended sediments suggested as the main sources.

In surface waters, in contrast to pCO<sub>2</sub> and POC data, we did not observe a positive correlation between DOC and the river discharge, in agreement with Brunet et al. (2009) who showed that DOC in the Nyong watershed was only flushed during a short period of time at the beginning of the short rainy season (Fig. 5). In contrast to POC, DOC did not peak a second time during the long rainy season (Fig. 5). We have no explanation to this, except the fact that this probable second flush of DOC was faster than our fortnightly sampling frequency. Nonetheless, DOC exhibited a similar seasonality in stream order 1 and high-order streams, but with a slight lag time due to the time the water needs to flow from upstream to downstream showing

630 that wetland from low-order streams are significant sources of C for downstream rivers. In addition, in the Awout River (order 3), a significant increase in DOC was observed at the beginning of the reflowing period indicating an additional source of DOC (Fig. 5). Actually, before the reflowing period, the bed of the Awout River was completely vegetated by large macrophytes (up to 2 m tall) and many small pockets of stagnating water remained. DOC could accumulate in these stagnating waters and be remobilized when the water flows again, as observed in temperate rivers (Deirmendjian et al., 2019; Sanders et al., 2007). The seasonal wetland flush in high-order streams can be also evidenced by peaks of TA during the long rainy seasons, while the increase in TA in streams orders 5 and 6 during the long dry seasons could not be explained by wetland inputs to river. In stream orders 5 and 6, during the long dry season, surface waters are likely fed by deeper groundwater, which are older and likely characterized by higher TA concentrations than shallower levels, as observed in temperate (Deirmendjian and Abril, 2018) and tropical (Duvert et al., 2020b) catchments. In the later study situated in a small tropical catchment in Australia, the authors gave additional evidence of a shift from biogenic (wetlands) to geogenic C source during dry seasons caused by changing water sources

### 4.3. C fluxes at the plot (first-order) and the watershed scales

At the first-order Mengong catchment scale, we estimated each fluxes of the stream C budget independently. C inputs from wetland ( $F_{WL}$ ) and non-flooded forest groundwater ( $F_{GW}$ ) to the stream contributed to 38% ( $4.0 \pm 1.5 \text{ tC yr}^{-1}$ ) and 62% ( $6.3 \pm 3.0$  645  $\text{tC yr}^{-1}$ ) of the total hydrological C inputs, respectively (Table 5; Fig. 7). However, when the later fluxes are weighed by respective surface area,  $F_{WL}$  and  $F_{GW}$  contributed to 73% ( $33.3 \pm 12.5 \text{ tC yr}^{-1}$ ) and 27% ( $13.1 \pm 6.2 \text{ tC yr}^{-1}$ ) of the total hydrological C inputs to the stream, respectively (Fig. 7). In the first-order Mengong catchment, 83% and 17% of the C degassing (58% and 42% if weighed by surface area) from the stream are sustained by inputs of DIC from non-flooded forest groundwater and wetland, respectively (Fig. 7). From our study design it was not possible to estimate these two contributions at the Nyong watershed scale. However, we might assume that the wetland contribution become greater with increasing stream order, particularly considering larger riparian wetlands in high-order streams and the development of floating macrophytes in river bed during dry seasons (Olivry, 1986). Nonetheless, our results are in line with the growing consensus that tropical wetlands contribute significantly to the C inputs in tropical rivers (Abril et al., 2014; Borges et al., 2015a, 2019, 2015b; Duvert et al., 2020a, 2020b). In the Mengong catchment, an important fraction (~50%) of the C entering the stream directly returns to 655 the atmosphere through degassing at the water-air interface (Fig. 7); the remaining C is transported, processed and further degassed downstream (Abril et al., 2014). In the Nyong watershed, our estimated  $k_{600}$  are typical of lowland tropical rivers (e.g., Alin et al., 2011; Borges et al., 2019) and their weak seasonality show that higher degassing rates during rainy seasons are rather a function of the increase of  $\text{CO}_2$  water-air gradient during rainy seasons - which is due to seasonal flush of wetland and macrophytes – rather than the increase in  $k_{600}$  usually observed during high water periods because of increasing water turbulence. In the Nyong watershed, heterotrophic respiration in the river (pelagic plus benthic) rate was  $99 \pm 27 \text{ mmol m}^{-2} \text{ d}^{-1}$  660 on average whereas the average  $\text{CO}_2$  degassing rate was  $1160 \pm 580 \text{ mmol m}^{-2} \text{ d}^{-1}$  (Table 6). This implies that only ~8.5% of

the degassing at the water-air interface was supported by heterotrophic respiration in the river. These rates are consistent with observations by Borges et al. (2019), who showed that, in the Congo basin, the heterotrophic respiration in the river averaged 81 mmol m<sup>-2</sup> d<sup>-1</sup> and represented ~11% of the average C degassing rate of 740 mmol m<sup>-2</sup> d<sup>-1</sup>. In the same way, heterotrophic  
665 respiration in the river accounts for less than 20% of the degassing flux from the Amazon Basin (Abril et al., 2014). Moreover, in the Nyong watershed, the ratio between C degassing rates and heterotrophic respiration in the river decreased in the stream order 5 (ratio of 6.5) compared to stream order 1 (ratio of 48) (Table 6). This is in line with the recent findings by Hotchkiss et al. (2015) in temperate rivers, where they showed that the contribution of internal metabolism to account for CO<sub>2</sub> emissions increased from upstream to downstream, or with the more recent findings by Borges et al. (2019) in the Congo basin who  
670 found a ratio of C degassing rates to heterotrophic respiration in the river of 29-137 and 3-17 in low-and high-order streams, respectively. These authors attributed their observations to the prevalence of lateral CO<sub>2</sub> inputs in sustaining CO<sub>2</sub> emissions.

In the Nyong watershed, about 6% (0.6±0.5 tC km<sup>-2</sup> yr<sup>-1</sup>), 69% (7.2±5.4 tC km<sup>-2</sup> yr<sup>-1</sup>) and 24% (2.5±2.3 tC km<sup>-2</sup> yr<sup>-1</sup>) of the F<sub>ocean</sub> occurs in the POC, DOC and DIC forms, respectively. These C exports to the ocean are consistent but slightly different  
675 from those reported by Meybeck (1993) for rivers in tropical humid regions, as he estimated that 20% (1.9 tC km<sup>-2</sup> yr<sup>-1</sup>), 53% (5.1 tC km<sup>-2</sup> yr<sup>-1</sup>) and 27% (2.6 tC km<sup>-2</sup> yr<sup>-1</sup>) occurs in the POC, DOC and DIC forms, respectively. Therefore, in the Nyong watershed, the export of DIC to the ocean was typical of humid tropical regions while the export of POC was lower and DOC was higher. In the Nyong watershed, lower POC export to the ocean might be explained by the low watershed slope and the negligible overland flow that limits soil erosion. In contrast, DOC concentration in the surface waters of the Nyong watershed  
680 was in the upper range of those reported for other African rivers (range is 50 to 4 270 µmol L<sup>-1</sup>; Tamooch et al. 2014 and references therein), thereby driving the higher DOC export to the ocean, which might be explained by higher wetland extent than in the other African rivers. Huang et al. (2012) estimated the quantity of C exported to the ocean from African tropical rivers (30°N-30°S) at 0.3, 1 and 0.6 tC km<sup>-2</sup> yr<sup>-1</sup> for the POC, DOC and DIC forms, respectively, but they did not partition these tropical rivers in humid or dry climates; our estimations of C export to the ocean were significantly higher for the tropical  
685 Nyong watershed located humid climate region. This shows the importance to upscale C fluxes for the same climatic regions, such as the widely used Koppen-Geiger climate classification system (Koppen, 1936) recently updated by Peel et al. (2007), otherwise upscaling might be strongly biased. In the Nyong watershed, the ratio between the C exported to the ocean and emitted to the atmosphere is 1:0.3, in agreement with ratio of 1:0.2 measured by Borges et al. (2015b) in the Congo River but contrasting with the global ratio of 1:1 estimated by Ciais et al. (2013) during the Fifth Assessment Report of the  
690 Intergovernmental Panel on Climate Change (IPCC). It shows that at least African rivers but probably all tropical rivers are strong emitters of C and therefore biogeochemical data in these rivers are urgently required to improve accuracy of regional and global C emission estimates from inland waters, and understand how they will respond to climate change (warming, change in hydrological cycle).

695 The integration of the different C fluxes can be done by comparing them with the terrestrial C budget. In the Mengong  
catchment, the total hydrological export of C ( $F_{GW}$ ,  $F_{GW-bis}$ ,  $F_{WL}$ ) represents ~3-5% of the catchment net C sink (range 201-336  
tC yr<sup>-1</sup>) (Fig. 7). This conclusion agrees with two plot studies in temperate ecosystems, which have shown that the hydrological  
export of C from forest ecosystems is ~3% (Deirmendjian et al., 2018; Kindler et al., 2011). In the Nyong watershed, the sum  
of the yearly C degassed ( $F_{degas}$ ) and hydrologically exported to the ocean ( $F_{ocean}$ ) represented ~10% of the net terrestrial C sink  
700 estimated by Brunet et al. (2009) (Table 8). This conclusion agrees with Duvert et al. (2020a), which showed that the C  
degassed and hydrologically exported at the river outlet represented ~7% of the local net terrestrial C sink in the small (140  
km<sup>2</sup>) tropical Howard catchment in Australia, ~20% if accounting to C losses via fire. In contrast, from a modelling approach  
in the entire Amazon watershed, Hastie et al. (2019) found that C degassed and hydrologically exported might represents 78%  
of the net terrestrial C sink. This is in line with findings of Abril et al. (2014) and Borges and al. (2019) who respectively found  
705 that C degassed from the Amazon and Congo watersheds was greater than the local net terrestrial C sink. Besides, Abril et al.  
(2014) attributed this C riverine C degassing to wetland C inputs as they showed that tropical wetland can hydrologically  
export 36-80% of their gross primary production (GPP) while terrestrial landscapes hydrologically export few percent of their  
net C sink, between 3% for forests and 13% from grasslands (Kindler et al., 2011). Altogether, this shows that in large  
watersheds such as the Amazon or the Congo rivers, fluvial C losses could offset more significantly the local net terrestrial C  
710 sink compared to relatively small tropical watersheds such as the Nyong or the Howard rivers, which is likely due to both more  
extensive wetland and greater hydrological fluxes in the Amazon and the Congo.

## Conclusions

In a first-order catchment, we showed here by determining all the terms of the C mass balance independently that attributing  
the whole amount of CO<sub>2</sub> emitted to the atmosphere and exported to the outlet to a unique terrestrial source and ignoring the  
river–wetland connectivity might lead to the misrepresentation of C dynamics in small tropical catchments and thus likely  
715 at larger scales. Indeed, in addition to the drainage of non-flooded forest groundwater to the stream, we highlighted the drainage  
and erosion of wetland as an important C source for the stream. Non-flooded forest groundwater was a significant source of C  
for surface waters, particularly for CO<sub>2</sub>, whereas in contrast, DOC and POC in surface waters were mainly provided by the  
drainage and erosion of wetlands. The flush of C from wetland to first-order streams is seasonally enhanced during rainy  
720 seasons when the connectivity with surface waters is greater, allowing the leaching of freshly and young OM to the stream,  
and thus increasing heterotrophic respiration in the river downstream. Nonetheless, at the Nyong watershed scale, the CO<sub>2</sub>  
emissions from the entire river network remained largely sustained by inputs of C from land and wetland, as heterotrophic  
respiration in the river represents only ~8.5% of the C degassing at the water-air interface. Moreover, at the Nyong watershed  
scale, we showed that the CO<sub>2</sub> degassed from the entire river network and the C hydrologically exported to the ocean might  
725 offset ~10% of the net terrestrial C sink estimated from the watershed. This study supports the view that African rivers are  
strong emitters of CO<sub>2</sub> to the atmosphere, mostly sustained by wetland inputs, and this must be better considered in global  
models.

## Data availability

If accepted the database will be publicly available at [zeonodo.org](https://zeonodo.org)

## 730 Competing interests

The authors declare they have no conflict of interest

## Acknowledgments

The Nyong Watershed is included in the CZO Multiscale TROPical CatchmentS (M-TROPICS, <https://mtropics.obs-mip.fr>), LMI PICASS-EAU (<https://picass-eau.ird.fr>), LMI DYCOFAC (<https://lab.ird.fr/collaboration/37/show>) and OZCAR  
735 (Critical Zone Observatories: Research and Application) funded by IRD (Research Institute for Development—Institut de Recherche sur le Développement) and INSU/CNRS. We thank our colleagues from IRGM (Yaoundé, Cameroon) involved in M-TROPICS for their help in the field and in the laboratory. M. M. was funded by the French Embassy in Cameroon (Mobility Fellowship) and L. D. by IRD (Post-Doctoral fellowship). This research was supported by IRD and by Strategic planning “PSIP Seq2C” (Interdisciplinary and Partnership Structuring Program on Continental Carbon Sequestration).

740

## References

- Abril, G. and Borges, A. V.: Carbon leaks from flooded land : do we need to re-plumb the inland water Ideas and perspectives : Carbon leaks from flooded land: do we need to replumb the inland water active pipe ?, *Biogeoscience*, 16, 769–784, doi:10.5194/bg-16-769-2019, 2019.
- 745 Abril, G., Martinez, J. M., Artigas, L. F., Moreira-Turcq, P., Benedetti, M. F., Vidal, L., Meziane, T., Kim, J. H., Bernardes, M. C., Savoye, N., Deborde, J., Souza, E. L., Albéric, P., Landim De Souza, M. F. and Roland, F.: Amazon River carbon dioxide outgassing fuelled by wetlands, *Nature*, 505(7483), 395–398, doi:10.1038/nature12797, 2014.
- Abril, G., Bouillon, S., Darchambeau, F., Teodoru, C. R., Marwick, T. R., Tamooch, F., Ochieng Omengo, F., Geeraert, N., Deirmendjian, L., Polsenaere, P. and Borges, A. V.: Technical note: Large overestimation of pCO<sub>2</sub> calculated from pH and alkalinity in acidic, organic-rich freshwaters, *Biogeosciences*, 12(1), 67–78, doi:10.5194/bg-12-67-2015, 2015.
- 750 Alin, S. R., Rasera, M. D. F. F. L., Salimon, C. I., Richey, J. E., Holtgrieve, G. W., Krusche, A. V. and Snidvongs, A.: Physical controls on carbon dioxide transfer velocity and flux in low-gradient river systems and implications for regional carbon budgets, *J. Geophys. Res. Biogeosciences*, 116(1), doi:10.1029/2010JG001398, 2011.
- Allen, G. H. and Pavelsky, T. M.: Global extent of rivers and streams, *Science* (80-. ), 361(6402), 585–588, doi:10.1126/science.aat0636, 2018.
- 755



- Amiotte Suchet, P., Probst, J. and Ludwig, W.: Worldwide distribution of continental rock lithology: Implications for the atmospheric / soil CO<sub>2</sub> uptake by continental weathering and alkalinity river transport to the oceans, *Global Biogeochem. Cycles*, 17(2), doi:10.1029/2002GB001891, 2003.
- Audry, S., Bessa, H. A., Bedimo, J.-P. B., Boeglin, J.-L., Boithias, L., Braun, J.-J., Dupré, B., Fauchaux, M., Lagane, C.,  
760 Maréchal, J.-C., Ndam-Ngoupayou, J. R., Nnomo, B. N., Nlozoa, J., Ntonga, J.-C., Ribolzi, O., Riotte, J., Rochelle-Newall, E. and Ruiz, L.: The Multiscale TROPICAL CatchmentS critical zone observatory M-TROPICS dataset I: The Nyong River Basin, Cameroon, *Hydrol. Process.*, 35(5), e14138, doi:10.1002/HYP.14138, 2021.
- Boeglin, J.-L., Ndam, J.-R. and Braun, J.-J.: Composition of the different reservoir waters in a tropical humid area: example of the Nsimi catchment (Southern Cameroon), *J. African Earth Sci.*, 37(1–2), 103–110, 2003.
- 765 Boeglin, J. ., Probst, J., Ndam-Ngoupayou, J., Nyeck, B., Etcheber, H., Mortatti, J. and Braun, J. .: Soil carbon stock and river carbon fluxes in humid tropical environments: the Nyong river basin (south Cameroon), in *Soil Erosion and Carbon Dynamics*, *Adv. Soil Sci*, pp. 275–288, CRC Press Boca Raton, Fla., 2005.
- Bolan, N. S., Adriano, D. C., Kunhikrishnan, A., James, T., Mcdowell, R. and Senesi, N.: *Dissolved Organic Matter*, 1st ed., Elsevier Inc., 2011.
- 770 Borges, A. V., Abril, G., Darchambeau, F., Teodoru, C. R., Deborde, J., Vidal, L. O., Lambert, T. and Bouillon, S.: Divergent biophysical controls of aquatic CO<sub>2</sub> and CH<sub>4</sub> in the World's two largest rivers, *Sci. Rep.*, 5, 15614, doi:https://doi.org/10.1038/srep15614, 2015a.
- Borges, A. V., Darchambeau, F., Lambert, T. and Morana, C.: Variations of dissolved greenhouse gases (CO<sub>2</sub>, CH<sub>4</sub>, N<sub>2</sub>O) in the Congo River network overwhelmingly driven by fluvial-wetland connectivity, *Biogeosciences*, 16(19), 3801–3834,  
775 doi:10.5194/bg-2019-68, 2019.
- Borges, A. V., Darchambeau, F., Teodoru, C. R., Marwick, T. R., Tamooch, F., Geeraert, N., Omengo, F. O., Guérin, F., Lambert, T., Morana, C., Okuku, E. and Bouillon, S.: Globally significant greenhouse-gas emissions from African inland waters, *Nat. Geosci.*, 8(8), 637–642, doi:10.1038/NGEO2486, 2015b.
- Braun, J.-J., Dupré, B., Viers, J., Ngoupayou, J. R. N., Bedimo, J.-P. B., Sigha-Nkamdjou, L., Freydier, R., Robain, H., Nyeck,  
780 B. and Bodin, J.: Biogeohydrodynamic in the forested humid tropical environment: the case study of the Nsimi small experimental watershed (south Cameroon), *Bull. la Société géologique Fr.*, 173(4), 347–357, 2002.
- Braun, J.-J., Ngoupayou, J. R. N., Viers, J., Dupre, B., Bedimo, J.-P. B., Boeglin, J.-L., Robain, H., Nyeck, B., Freydier, R. and Nkamdjou, L. S.: Present weathering rates in a humid tropical watershed: Nsimi, South Cameroon, *Geochim. Cosmochim. Acta*, 69(2), 357–387, 2005.
- 785 Braun, J.-J., Marechal, J.-C., Riotte, J., Boeglin, J.-L., Bedimo, J.-P. B., Ngoupayou, J. R. N., Nyeck, B., Robain, H., Sekhar, M. and Audry, S.: Elemental weathering fluxes and saprolite production rate in a Central African lateritic terrain (Nsimi, South Cameroon), *Geochim. Cosmochim. Acta*, 99, 243–270, 2012.
- Brunet, F., Dubois, K., Veizer, J., Ndong, G. R. N., Ngoupayou, J. R. N., Boeglin, J. L. and Probst, J. L.: Terrestrial and fluvial carbon fluxes in a tropical watershed: Nyong basin, Cameroon, *Chem. Geol.*, 265(3), 563–572,

- 790 doi:<https://doi.org/10.1016/j.chemgeo.2009.05.020>, 2009.
- Camino-Serrano, M., ... B. G.-G. and 2014, undefined: Linking variability in soil solution dissolved organic carbon to climate, soil type, and vegetation type, *Wiley Online Libr.*, 28(5), 497–509, doi:10.1002/2013GB004726, 2014.
- Cardoso, S. J., Enrich-Prast, A., Pace, M. L. and Roland, F.: Do models of organic carbon mineralization extrapolate to warmer tropical sediments?, *Limnol. Oceanogr.*, 59(1), 48–54, 2014.
- 795 Ciais, P., Sabine, C., Bala, G., Bopp, L., Brovkin, V., Canadell, J. G., Chhabra, A., Defries, R., Galloway, J., Heimann, M., Jones, C., Le Quéré, C., Myeni, R., Piao, S. and Thornton, P.: *Carbon and Other Biogeochemical Cycles.*, 2013.
- Cole, J. J., Prairie, Y. T., Caraco, N. F., McDowell, W. H., Tranvik, L. J., Striegl, R. G., Duarte, C. M., Kortelainen, P., Downing, J. A., Middelburg, J. J. and Melack, J.: Plumbing the Global Carbon Cycle : Integrating Inland Waters into the Terrestrial Carbon Budget, *Ecosystems*, 10(1), 172–185, doi:10.1007/s10021-006-9013-8, 2007.
- 800 Davidson, E. A., Verchot, L. V., Cattânio, J. H., Ackerman, I. L. and Carvalho, J. E. M.: Effects of soil water content on soil respiration in forests and cattle pastures of eastern Amazonia, *Biogeochemistry*, 48, 53–69, 2000.
- Deirmendjian, L. and Abril, G.: Carbon dioxide degassing at the groundwater-stream-atmosphere interface : isotopic equilibration and hydrological mass balance in a sandy watershed, *J. Hydrol.*, 558, 129–143, doi:10.1016/j.jhydrol.2018.01.003, 2018.
- 805 Deirmendjian, L., Loustau, D., Augusto, L., Lafont, S., Chipeaux, C., Poirier, D. and Abril, G.: Hydro-ecological controls on dissolved carbon dynamics in groundwater and export to streams in a temperate pine forest, *Biogeosciences*, 15(2), 669–691, doi:10.5194/bg-15-669-2018, 2018.
- Deirmendjian, L., Anschutz, P., Morel, C., Mollier, A., Augusto, L., Loustau, D., Cotovicz, L. C., Buquet, D., Lajaunie, K., Chaillou, G., Voltz, B., Charbonnier, C., Poirier, D. and Abril, G.: Importance of the vegetation-groundwater-stream
- 810 continuum to understand transformation of biogenic carbon in aquatic systems – A case study based on a pine-maize comparison in a lowland sandy watershed (Landes de Gascogne, SW France), *Sci. Total Environ.*, doi:10.1016/j.scitotenv.2019.01.152, 2019.
- Drake, T. W., Raymond, P. A. and Spencer, R. G. M.: Terrestrial carbon inputs to inland waters: A current synthesis of estimates and uncertainty, *Limnol. Oceanogr. Lett.*, 3(3), 132–142, doi:10.1002/lol2.10055, 2018.
- 815 Duvert, C., Hutley, L. B., Beringer, J., Bird, M. I., Birkel, C., Maher, D. T., Northwood, M., Rudge, M., Setterfield, S. A. and Wynn, J. G.: Net landscape carbon balance of a tropical savanna: Relative importance of fire and aquatic export in offsetting terrestrial production, *Glob. Chang. Biol.*, 26(10), 5899–5913, doi:10.1111/GCB.15287, 2020a.
- Duvert, C., Hutley, L. B., Birkel, C., Rudge, M., Munksgaard, N. C., Wynn, J. G., Setterfield, S. A., Cendón, D. I. and Bird, M. I.: Seasonal shift from biogenic to geogenic fluvial carbon caused by changing water sources in the wet-dry tropics, *J.*
- 820 *Geophys. Res. Biogeosciences*, 125(2), e2019JG005384, 2020b.
- Engle, diana I., Melack, J. m, Doyle, robert D. and fisher, T. r: High rates of net primary production and turnover of floating grasses on the Amazon floodplain: implications for aquatic respiration and regional CO<sub>2</sub> flux, *Glob. Chang. Biol.*, 14(2), 369–381, doi:10.1111/J.1365-2486.2007.01481.X, 2008.

- Fang, W., Wei, Y., Liu, J., Kosson, D., Management, H. van der S.-W. and 2016, U.: Effects of aerobic and anaerobic biological processes on leaching of heavy metals from soil amended with sewage sludge compost, *Elsevier, Waste mana*(58), 324–334, 2016.
- Friedlingstein, P., O’Sullivan, M., Jones, M. W., Andrew, R. M., Hauck, J., Olsen, A., Peters, G. P., Peters, W., Pongratz, J., Sitch, S., Le Quéré, C., Canadell, J. G., Ciais, P., Jackson, R. B., Alin, S., Aragão, L. E. O. C., Arneeth, A., Arora, V., Bates, N. R., Becker, M., Benoit-Cattin, A., Bittig, H. C., Bopp, L., Bultan, S., Chandra, N., Chevallier, F., Chini, L. P., Evans, W., Florentie, L., Forster, P. M., Gasser, T., Gehlen, M., Gilfillan, D., Gkritzalis, T., Gregor, L., Gruber, N., Harris, I., Hartung, K., Haverd, V., Houghton, R. A., Ilyina, T., Jain, A. K., Joetzjer, E., Kadono, K., Kato, E., Kitidis, V., Korsbakken, J. I., Landschützer, P., Lefèvre, N., Lenton, A., Lienert, S., Liu, Z., Lombardozzi, D., Marland, G., Metzl, N., Munro, D. R., Nabel, J. E. M. S., Nakaoka, S. I., Niwa, Y., O’Brien, K., Ono, T., Palmer, P. I., Pierrot, D., Poulter, B., Resplandy, L., Robertson, E., Rödenbeck, C., Schwinger, J., Séférian, R., Skjelvan, I., Smith, A. J. P., Sutton, A. J., Tanhua, T., Tans, P. P., Tian, H., Tilbrook, B., Van Der Werf, G., Vuichard, N., Walker, A. P., Wanninkhof, R., Watson, A. J., Willis, D., Wiltshire, A. J., Yuan, W., Yue, X. and Zaehle, S.: Global Carbon Budget 2020, *Earth Syst. Sci. Data*, 12(4), 3269–3340, doi:10.5194/ESSD-12-3269-2020, 2020.
- Gaillardet, J., Braud, I., Hankard, F., Anquetin, S., Bour, O., Dorfliger, N., de Dreuz, J. R., Galle, S., Galy, C., Gogo, S., Gourcy, L., Habets, F., Laggoun, F., Longuevergne, L., Le Borgne, T., Naaim-Bouvet, F., Nord, G., Simonneaux, V., Six, D., Talleg, T., Valentin, C., Abril, G., Allemand, P., Arènes, A., Arfib, B., Arnaud, L., Arnaud, N., Arnaud, P., Audry, S., Comte, V. B., Batiot, C., Battais, A., Bellot, H., Bernard, E., Bertrand, C., Bessière, H., Binet, S., Bodin, J., Bodin, X., Boithias, L., Bouchez, J., Boudevillain, B., Moussa, I. B., Branger, F., Braun, J. J., Brunet, P., Caceres, B., Calmels, D., Cappelaere, B., Celle-Jeanton, H., Chabaux, F., Chalikakis, K., Champollion, C., Copard, Y., Cotel, C., Davy, P., Deline, P., Delrieu, G., Demarty, J., Dessert, C., Dumont, M., Emblanch, C., Ezzahar, J., Estèves, M., Favier, V., Fauchaux, M., Filizola, N., Flammarion, P., Floury, P., Fovet, O., Fournier, M., Francez, A. J., Gandois, L., Gascuel, C., Gayer, E., Genthon, C., Gérard, M. F., Gilbert, D., Gouttevin, I., Grippa, M., Gruau, G., Jardani, A., Jeanneau, L., Join, J. L., Jourde, H., Karbou, F., Labat, D., Lagadeuc, Y., Lajeunesse, E., Lastennet, R., Lavado, W., Lawin, E., Lebel, T., Le Bouteiller, C., Legout, C., Lejeune, Y., Le Meur, E., Le Moigne, N., Lions, J., et al.: OZCAR: The French Network of Critical Zone Observatories, *Vadose Zo. J.*, 17(1), 180067, doi:10.2136/VZJ2018.04.0067, 2018.
- Geeraert, N., Omengo, F. O., Borges, A. V., Govers, G. and Bouillon, S.: Shifts in the carbon dynamics in a tropical lowland river system (Tana River, Kenya) during flooded and non-flooded conditions, *Biogeochemistry*, 132(1–2), 141–163, doi:10.1007/s10533-017-0292-2, 2017.
- Gómez-Gener, L., Rocher-Ros, G., Battin, T., Cohen, M. J., Dalmagro, H. J., Dinsmore, K. J., Drake, T. W., Duvert, C., Enrich-Prast, A., Horgby, Å., Johnson, M. S., Kirk, L., Machado-Silva, F., Marzolf, N. S., McDowell, M. J., McDowell, W. H., Miettinen, H., Ojala, A. K., Peter, H., Pumpanen, J., Ran, L., Riveros-Iregui, D. A., Santos, I. R., Six, J., Stanley, E. H., Wallin, M. B., White, S. A. and Sponseller, R. A.: Global carbon dioxide efflux from rivers enhanced by high nocturnal emissions, *Nat. Geosci.*, 14(5), 289–294, doi:10.1038/S41561-021-00722-3, 2021.

- Gran, G.: Determination of the equivalence point in potentiometric titrations. Part II, *Analyst*, 77(920), 661–671, 1952.
- Gumbrecht, T., Román-Cuesta, R. M., Verchot, L. V., Herold, M., Wittmann, F., Householder, E., Herold, N. and Murdiyarso, D.: Tropical and Subtropical Wetlands Distribution version 2, , doi:doi:10.17528/CIFOR/DATA.00058, 2017.
- 860 Haase, K. and Rättsch, G.: The morphology and anatomy of tree roots and their aeration strategies, in *Amazonian Floodplain Forests*, pp. 141–161, Springer., 2010.
- Hagedorn, F., Bruderhofer, N., Ferrari, A. and Niklaus, P. A.: Tracking litter-derived dissolved organic matter along a soil chronosequence using <sup>14</sup>C imaging: Biodegradation, physico-chemical retention or preferential flow?, *Soil Biol. Biochem.*, 88, 333–343, doi:10.1016/J.SOILBIO.2015.06.014, 2015.
- 865 Hastie, A., Lauerwald, R., Ciais, P. and Regnier, P.: Aquatic carbon fluxes dampen the overall variation of net ecosystem productivity in the Amazon basin: An analysis of the interannual variability in the boundless, *Wiley Online Libr.*, 25(6), 2094–2111, doi:10.1111/gcb.14620, 2019.
- Holgerson, M. A. and Raymond, P. A.: Large contribution to inland water CO<sub>2</sub> and CH<sub>4</sub> emissions from very small ponds, , 9(February), doi:10.1038/NGEO2654, 2016.
- 870 Hotchkiss, E. R., Jr, R. O. H., Sponseller, R. A., Butman, D., Klaminder, J., Laudon, H., Rosvall, M. and Information, S.: Sources of and processes controlling CO<sub>2</sub> emissions change with the size of streams and rivers, *Nat. Geosci.*, 8(9), 696–699, doi:10.1038/NGEO2507, 2015.
- Huang, T., Fu, Y., Pan, P. and Chen, C.: Fluvial carbon fluxes in tropical rivers, *Curr. Opin. Environ. Sustain.*, 4(2), 162–169, 875 2012.
- Huang, Y., Evaristo, J. and Li, Z.: Multiple tracers reveal different groundwater recharge mechanisms in deep loess deposits, *Elsevier*, 353, 204–212, 2019.
- Johnson, M. S., Lehmann, Æ. J., Couto, E., Filho, J. and Riha, S.: DOC and DIC in flowpaths of Amazonian headwater catchments with hydrologically contrasting soils, *Biogeochemistry*, 81, 45–57, doi:10.1007/s10533-006-9029-3, 2006.
- 880 Johnson, M. S., Lehmann, J., Riha, S. J., Krusche, A. V., Richey, J. E., Ometto, J. P. H. B. and Couto, E. G.: CO<sub>2</sub> efflux from Amazonian headwater streams represents a significant fate for deep soil respiration, *Geophys. Res. Lett.*, 35(17), doi:10.1029/2008GL034619, 2008.
- Jones, M. B. and Humphries, S. W.: Impacts of the C<sub>4</sub> sedge *Cyperus papyrus* L. on carbon and water fluxes in an African wetland, , 107–113, 2002.
- 885 Junk, W., Bayley, P. and Sparks, R.: The flood pulse concept in river-floodplain system.pdf, *Can. Spec. Publ. Fish. Aquat. Sci.*, 106(1), 110–127, 1989.
- Kaiser, K., Guggenberger, G. and Zech, W.: Sorption of DOM and DOM fractions to forest soils, *Geoderma*, 74(3–4), 281–303, doi:10.1016/S0016-7061(96)00071-7, 1996.
- Kalbitz, K. and Kaiser, K.: Contribution of dissolved organic matter to carbon storage in forest mineral soils, *J. Plant Nutr. Soil Sci.*, 171(1), 52–60, doi:10.1002/JPLN.200700043, 2008.
- 890 Kalbitz, K., Solinger, S., Park, J., Michalzik, B. and Matzner, E.: Controls on the dynamics of dissolved organic matter in

- soils: a review, *Soil Sci.*, 165(4), 277–304, 2000.
- Kalbitz, K., Schwesig, D., Rethemeyer, J. and Matzner, E.: Stabilization of dissolved organic matter by sorption to the mineral soil, *Soil Biol. Biochem.*, 37(7), 1319–1331, doi:10.1016/J.SOILBIO.2004.11.028, 2005.
- 895 Kindler, R., Siemens, J., ... K. K.-G. C. and 2011, undefined: Dissolved carbon leaching from soil is a crucial component of the net ecosystem carbon balance, *Wiley Online Libr.*, 17(2), 1167–1185, doi:10.1111/j.1365-2486.2010.02282.x, 2011.
- Koppen, W.: *Das geographische System der Klimate*, in *Handbuch der Klimatologie*, edited by B. Köppen, W. and Geiger, G., I. C. Gebr, pp. 1–44., 1936.
- Kothawala, D. N., Moore, T. R. and Hendershot, W. H.: Soil Properties Controlling the Adsorption of Dissolved Organic  
 900 Carbon to Mineral Soils, *Soil Sci. Soc. Am. J.*, 73(6), 1831–1842, doi:10.2136/SSSAJ2008.0254, 2009.
- Lambert, T., Bouillon, S., Darchambeau, F., Massicotte, P. and Borges, A. V: Shift in the chemical composition of dissolved organic matter in the Congo River network, *Biogeosciences*, 13(18), 5405–5420, doi:10.5194/bg-13-5405-2016, 2016.
- Lauerwald, R., Laruelle, G. G., Hartmann, J., Ciais, P. and Regnier, P. A. G.: Spatial patterns in CO<sub>2</sub> evasion from the global river network, *Global Biogeochem. Cycles*, 29(5), 534–554, doi:10.1002/2014GB004941, 2015.
- 905 Lehner, B., Verdin, K., Jarvis, A. and Systems, E.: New global hydrography derived from spaceborne elevation data, *Eos, Trans. Am. Geophys. Union*, 89(10), 93–94, 2008.
- Lewis, E. and Wallace Upton, N.: Program developed for CO<sub>2</sub> calculations, , doi:10.2172/639712, 1998.
- Ludwig, W., Probst, J. and Kempe, S.: Predicting the oceanic input of organic carbon by continental erosion, *Global Biogeochem. Cycles*, 10(1), 23–41, 1996.
- 910 Malard, F. and Hervant, F.: Oxygen supply and the adaptations of animals in groundwater, *Freshw. Biol.*, 41(1), 1–30, doi:10.1046/J.1365-2427.1999.00379.X, 1999.
- Maréchal, J., Braun, J., Riotte, J., Bedimo, J. B. and Boeglin, J.: Hydrological processes of a rainforest headwater swamp from natural chemical tracing in Nsimi watershed, Cameroon, *Hydrol. Process.*, 25(14), 2246–2260, 2011.
- Mayorga, E., Aufdenkampe, A. K., Masiello, C. A., Krusche, A. V, Hedges, J. I., Quay, P. D., Richey, J. E. and Brown, T. A.:  
 915 Young organic matter as a source of carbon dioxide outgassing from Amazonian rivers, , doi:10.1038/nature03880, 2005.
- Meybeck, M.: Carbon, nitrogen, and phosphorus transport by world rivers, *Am. J. Sci.*, 282(4), 401–450, 1982.
- Meybeck, M.: Global chemical weathering of surficial rocks estimated from river dissolved loads, *Am. J. Sci.*, 287(5), 401–428, doi:10.2475/ajs.287.5.401, 1987.
- Meybeck, M.: Riverine transport of atmospheric carbon: Sources, global typology and budget, *Water, Air, Soil Pollut.*, 70(1–  
 920 4), 443–463, doi:10.1007/BF01105015, 1993.
- Millero, F. J.: The thermodynamics of the carbonate system in seawater, *Geochem. Cosmochim. Ac.*, 43, 1651–1661, 1979.
- Mitsch, W. J., Zhang, L., Stefanik, K. C., Nahlik, A. M., Anderson, C. J., Bernal, B., Hernandez, M. and Song, K.: Creating Wetlands: Primary Succession, Water Quality Changes, and Self-Design over 15 Years, *Bioscience*, 62(3), 237–250, doi:10.1525/BIO.2012.62.3.5, 2012.
- 925 Moore, T. R.: Dissolved organic carbon in a northern boreal landscape, *Global Biogeochem. Cycles*, 17(4),

doi:10.1029/2003GB002050, 2003.

Moreira-Turcq, P., Bonnet, M. P., Amorim, M., Bernardes, M., Lagane, C., Maurice, L., Perez, M. and Seyler, P.: Seasonal variability in concentration, composition, age, and fluxes of particulate organic carbon exchanged between the floodplain and Amazon River, *Global Biogeochem. Cycles*, 27(1), 119–130, doi:10.1002/gbc.20022, 2013.

- 930 Neff, J. and Asner, G.: Dissolved organic carbon in terrestrial ecosystems: synthesis and a model, *Springer*, 4(1), 29–48, doi:10.1007/s100210000058, 2001.

Nkoue-ndondo, G.-R.: Le cycle du carbone en domaine tropical humide: exemple du bassin versant forestier du Nyong au sud Cameroun, Université de Toulouse, Université Toulouse III-Paul Sabatier., 2008.

- Nkoue Ndong, G. R., Probst, J.-L. L., Ndjama, J., Ndam Ngoupayou, J. R., Boeglin, J.-L. L., Takem, G. E., Brunet, F.,  
935 Mortatti, J., Gauthier-Lafaye, F., Braun, J.-J. J., Ekodeck, G. E., Nkoue-ndondo, G.-R., Probst, J.-L. L., Ndjama, J., Ngoupayou, J. R. N., Boeglin, J.-L. L., Takem, G. E., Brunet, F., Mortatti, J., Gauthier-Lafaye, F. and Braun, J.-J. J.: Stable Carbon Isotopes  $\delta^{13}\text{C}$  as a Proxy for Characterizing Carbon Sources and Processes in a Small Tropical Headwater Catchment: Nsimi, Cameroon, *Aquat. Geochemistry*, 1–30, doi:10.1007/s10498-020-09386-8, 2020.

- Nyeck, B., Bilong, P., Monkam, A. and Belinga, S. M. E.: Mise au point d'un modèle de cartographie et de classification des  
940 sols en zone forestières intertropicale au Cameroun. Cas du plateau forestier humide de Zoétélé, Géocam2, Press Uni. Yaoundé, 171–180, 1999.

Oliva, P., Viers, J., Dupré, B., Fortuné, J., Martin, F., Braun, J., Nahon, D. and Robain, H.: The effect of organic matter on chemical weathering: Study of a small tropical watershed: Nsimi-Zoetele site, Cameroon, *Geochim. Cosmochim. Acta*, 63(23–24), 4013–4055, 1999.

- 945 Olivry, J.: Fleuves et rivières du Cameroun, edited by ORSTOM, Paris., 1986.

Peel, M. C., Finlayson, B. L. and McMahon, T. A.: Updated world map of the Köppen-Geiger climate classification, *Hydrol. Earth Syst. Sci.*, 11(5), 1633–1644, doi:10.5194/hess-11-1633-2007, 2007.

Piedade, M. T. F., Ferreira, C. S., de Oliveira Wittmann, A., Buckeridge, M. and Parolin, P.: Biochemistry of Amazonian floodplain trees, in *Amazonian floodplain forests*, pp. 127–139, Springer., 2010.

- 950 Raymond, P. A., Zappa, C. J., Butman, D., Bott, T. L., Potter, J., Mulholland, P., Laursen, A. E., McDowell, W. H. and Newbold, D.: Scaling the gas transfer velocity and hydraulic geometry in streams and small rivers, *Limnol. Oceanogr. Fluids Environ.*, 2(1), 41–53, doi:10.1215/21573689-1597669, 2012.

- Raymond, P. A., Hartmann, J., Lauerwald, R., Sobek, S., McDonald, C., Hoover, M., Butman, D., Striegl, R., Mayorga, E., Humborg, C., Kortelainen, P., Dürr, H., Meybeck, M., Ciais, P. and Guth, P.: Global carbon dioxide emissions from inland  
955 waters, *Nature*, 503(7476), 355–359, doi:10.1038/nature12760, 2013.

Sabater, S., Armengol, J., Comas, E., Sabater, F., Urrizalqui, I. and Urrutia, I.: Algal biomass in a disturbed Atlantic river: water quality relationships and environmental implications, *Sci. Total Environ.*, 263(1–3), 185–195, doi:10.1016/S0048-9697(00)00702-6, 2000.

Sanderman, J. and Amundson, R.: A comparative study of dissolved organic carbon transport and stabilization in California

- 960 forest and grassland soils, *Biogeochemistry*, 89(3), 309–327, doi:10.1007/S10533-008-9221-8, 2008.
- Sanders, I. A., Cotton, J., Hildrew, A. G. and Trimmer, M.: Emission of Methane from Chalk Streams Has Potential Implications for Agricultural Practices, *Freshw. Biol.*, 52(6), 1176–1186, doi:10.1111/j.1365-2427.2007.01745.x, 2007.
- Sauer, D., Sommer, M., Jahn, R., Sauer, D., Sponagel, H., Sommer, M., Giani, L., Jahn, R. and Stahr, K.: Podzol : Soil of the Year 2007 . A review on its genesis , occurrence , and functions A review on its genesis , occurrence , and functions, *J. Plant*
- 965 *Nutr. Soil Sci.*, 170(5), 581–597, doi:10.1002/jpln.200700135, 2007.
- Saunders, M. J., Jones, M. B. and Kansime, F.: Carbon and water cycles in tropical papyrus wetlands, *Wetl. Ecol. Manag.*, 15(6), 489–498, doi:10.1007/s11273-007-9051-9, 2007.
- Saunois, M., Stavert, A. R., Poulter, B., Bousquet, P., Canadell, J. G., Jackson, R. B., Raymond, P. A., Dlugokencky, E. J., Houweling, S., Patra, P. K., Ciais, P., Arora, V. K., Bastviken, D., Bergamaschi, P., Blake, D. R., Brailsford, G., Bruhwiler,
- 970 L., Carlson, K. M., Carrol, M., Castaldi, S., Chandra, N., Crevoisier, C., Crill, P. M., Covey, K., Curry, C. L., Etiope, G., Frankenberg, C., Gedney, N., Hegglin, M. I., Höglund-Isakson, L., Hugelius, G., Ishizawa, M., Ito, A., Janssens-Maenhout, G., Jensen, K. M., Joos, F., Kleinen, T., Krummel, P. B., Langenfelds, R. L., Laruelle, G. G., Liu, L., Machida, T., Maksyutov, S., McDonald, K. C., McNorton, J., Miller, P. A., Melton, J. R., Morino, I., Müller, J., Murgia-Flores, F., Naik, V., Niwa, Y., Noce, S., O&apos;Doherty, S., Parker, R. J., Peng, C., Peng, S., Peters, G. P., Prigent, C., Prinn, R., Ramonet, M., Regnier,
- 975 P., Riley, W. J., Rosentreter, J. A., Segers, A., Simpson, I. J., Shi, H., Smith, S. J., Steele, P. L., Thornton, B. F., Tian, H., Tohjima, Y., Tubiello, F. N., Tsuruta, A., Viovy, N., Voulgarakis, A., Weber, T. S., van Weele, M., van der Werf, G. R., Weiss, R. F., Worthy, D., Wunch, D., Yin, Y., Yoshida, Y., Zhang, W., Zhang, Z., Zhao, Y., Zheng, B., Zhu, Q., Zhu, Q. and Zhuang, Q.: The Global Methane Budget 2000&ndash;2017, *Earth Syst. Sci. Data Discuss.*, doi:10.5194/essd-2019-128, 2019.
- Sawakuchi, H. O., Neu, V., Ward, N. D., Barros, M. D. L. C., Valerio, A. M., Gagne-Maynard, W., Cunha, A. C., Less, D. F.
- 980 S. S., Diniz, J. E. M., Brito, D. C., Krusche, A. V. and Richey, J. E.: Carbon dioxide emissions along the lower Amazon River, *Front. Mar. Sci.*, 4(March), 1–12, doi:10.3389/fmars.2017.00076, 2017.
- Shen, Y., Chapelle, F. H., Strom, E. W. and Benner, R.: Origins and bioavailability of dissolved organic matter in groundwater, , 61–78, doi:10.1007/s10533-014-0029-4, 2015.
- Silva, T. S. F., Melack, J. M. and Novo, E. M. L. M.: Responses of aquatic macrophyte cover and productivity to flooding
- 985 variability on the Amazon floodplain, *Glob. Chang. Biol.*, 19(11), 3379–3389, doi:10.1111/GCB.12308, 2013.
- Strahler, A. N.: Mtm Quantitative Analysis of Watershed Geomorphology, *Trans. Am. Geophys. Union*, 38(6), 913–920, 1957.
- Suchel, J.-B.: Les climats du Cameroun, Université de Bordeaux III, France., 1987.
- Tamooch, F., Van Den Meersche, K., Meysman, F., Marwick, T. R., Borges, A. V., Merckx, R., Dehairs, F., Schmidt, S., Nyunja, J. and Bouillon, S.: Distribution and origin of suspended matter and organic carbon pools in the Tana River Basin, Kenya,
- 990 *Biogeosciences*, 9(8), 2905–2920, doi:10.5194/bg-9-2905-2012, 2012.
- Tamooch, F., Meysman, F. J. R., Borges, A. V., Marwick, T. R., Van, K., Meersche, D., Dehairs, F., Merckx, R. and Bouillon, S.: Sediment and carbon fluxes along a longitudinal gradient in the lower Tana River (Kenya), *Biogeosciences*, 119(7), 1340–1353, doi:10.1002/2013JG002358, 2014.

- Viers, J., Dupré, B., Polvé, M., Schott, J., Dandurand, J. L. and Braun, J. J.: Chemical weathering in the drainage basin of a tropical watershed (Nsimi-Zoetele site, Cameroon) : comparison between organic-poor and organic-rich waters, *Chem. Geol.*, 140(3–4), 181–206, doi:10.1016/S0009-2541(97)00048-X, 1997.
- Viers, J., Dupré, B., Braun, J. J., Deberdt, S., Angeletti, B., Ngoupayou, J. N. and Michard, A.: Major and trace element abundances, and strontium isotopes in the Nyong basin rivers (Cameroon): constraints on chemical weathering processes and elements transport mechanisms in humid tropical environments, *Chem. Geol.*, 169(1–2), 211–241, doi:10.1016/S0009-2541(00)00298-9, 2000.
- Weiss, R. F.: Carbon dioxide in water and seawater: the solubility of a non-ideal gas, *Mar. Chem.*, doi:10.1016/0304-4203(74)90015-2, 1974.
- White, A. F. and Blum, A. E.: Effects of climate on chemical\_ weathering in watersheds, *Geochim. Cosmochim. Acta*, 59(9), 1729–1747, 1995.



Rivers	<i>Mengong</i>	<i>Mengong</i>	<i>Awout</i>	<i>So'o</i>	<i>Nyong</i>	<i>Nyong</i>
Stations	Source	Outlet	Messam	Pont So'o	Mbalmayo	Olama
Latitude	3.17°N	3.17°N	3.28°N	3.32°N	3.52°N	3.43°N
Longitude	11.83°E	11.83°E	11.78°E	11.48° E	11.5°E	11.28°E
Gauging station	No	Yes	Yes	Yes	Yes	Yes
Altitude (m)	680	669	647	634	634	628
Catchment area (km <sup>2</sup> )	0.48	0.6	206	3070	13,555	18,510
Wetlands (%)		20	5.7	5.3	4.6	4.4
Catchment slope (‰)	1.3	1.3	1.2	1.1	0.16	0.15
Stream order	groundwater	1	3	4	5	6
Averaged-annual river flow in 2016 (m <sup>3</sup> s <sup>-1</sup> )	0.00544 <sup>a</sup>	0.009±0.002	3.9±4.8	35.6±40.6	146±112	195±160
Averaged-annual rainfall (mm yr <sup>-1</sup> )	1986					

**Table 1: geographical and hydrological catchments characteristics.** <sup>a</sup> represents  $Q_{hill}$  (Fig. 3) and it is estimated from Eq. 1.

Parameters	T	pH	Specific conductivity	Oxygen saturation	TSM
Units	°C	Unitless	μS cm <sup>-1</sup>	%	mg L <sup>-1</sup>
Mengong wetland <sup>a</sup>	24.2±1.4 [21.9-26.3]	5.5±0.6 [4.9-6.6]			
Mengong source	23.2±0.1 [23~23.6]	5.0±0.1 [4.6~5.3]	15.1±0.8 [14.1~17.4]	50±8 [38~68]	
Mengong outlet (order 1)	22.9±0.7 [21.9~24.4]	5.6±0.2 [5.3~6.0]	16.7±4.5 [5.2~24.7]	50±9 [23~62]	5.3±2.1 [1.8~11.1]
Awout (order 3)	22.5±0.5 [22~23.5]	5.6±0.2 [5.0~6.1]	21.6±5.5 [16.5~40.3]	47±9 [37~67]	10.4±6.1 [4.9~27.5]
So'o (order 4)	23.9±1.3 [22.4~27.6]	6.1±0.2 [5.7~6.6]	23.4±5.0 [18.3~35]	57±6 [46~69]	14.4±3.8 [8.2~22.9]
Nyong (Mbalamayo, order 5)	26.1±1.3 [24.3~29.0]	6.2±0.3 [5.5~6.9]	36.6±19 [19.6~86.3]	40±20 [13~81]	8.9±2.0 [4.3~12.0]
Nyong (Olama, order 6)	25.7±1.4 [24.1~28.8]	6.2±0.3 [5.5~6.6]	31.4±12.8 [20.1~69.3]	43±12 [24~67]	9.7±3.2 [3.7~14.8]

1010

**Table 2: Spatial distribution of physicochemical parameters (yearly average±standard deviation) in waters of the Nyong watershed during the sampling year 2016. The range is shown in square brackets. <sup>a</sup> was measured in the topsoil solution of the Mengong wetland at 0.4 m depth by Nkoue-Ndondo et al. (2020).**

Parameters	pCO <sub>2</sub>	TA	DIC	DOC	POC	POC
Units	ppmv	μmol L <sup>-1</sup>	μmol L <sup>-1</sup>	μmol L <sup>-1</sup>	%	μmol L <sup>-1</sup>
Mengong wetland	36 840±23 190 <sup>a</sup> [3 900-84 240]	122±46 <sup>a</sup> [50-216]	1 430±900 <sup>a</sup> [150-3 270]	1 420±750 <sup>b</sup> [1 250 - 2 920]		
Mengong source	78 800±40 110 [12 700~209 000]	53±26 [15~138]	2 940±1 485 [500~7 560]	83		
Mengong outlet (order 1)	15 600±8 900 [3 980~41 000]	90± 36 [20~156]	670±360 [170~1 710]	1 925±970 [1 090~4 150]	23±5 [14~26]	101±44 [14~213]
Awout (order 3)	15 400±7 300 [5 760~26 710]	67±39 [11~166]	670±315 [260~1 170]	3 200±1 840 [2 000~7 550]	16±3 [11~21]	130±50 [72~243]
So'o (order 4)	12 700±5 100 [4 900~23 200]	74±34 [10~145]	670±260 [300~1 320]	2 170±980 [1 100~5 320]	18±4 [12~29]	210±60 [125~360]
Nyong (Mbalamayo, order 5)	11 800±5 100 [3 620~22 460]	123±63 [20~230]	720±270 [220~1 200]	2 000±860 [1 020~5 300]	20±3 [16~26]	150±40 [62~220]
Nyong (Olama, order 6)	11 000±5 550 [3 000~21 700]	134±70 [10~265]	640±330 [170~1 240]	1 860±440 [1 100~2 880]	18±2 [15~23]	150±50 [55~235]

1015

**Table 3: Spatial distribution of C variables (yearly average±standard deviation) in waters of the Nyong watershed during the sampling year 2016. The range is shown in square brackets. <sup>a</sup>measured in the topsoil solution of the Mengong wetland at 0.4 m depth by Nkoue-Ndondo et al. (2020). <sup>b</sup> measured in the topsoil solution of the Mengong wetland at 0.4 m depth by Braun et et al. (2005).**

1020

	Mengong Discharge	Awout Discharge	So'o Discharge	Nyong at Mbalmayo Discharge	Nyong at Olama Discharge
Oxygen saturation			-0.5	-0.8	-0.8
pH			-0.5	-0.7	-0.7
Specific conductivity			-0.5	-0.6	-0.6
TA			-0.4	-0.4	-0.4
pCO <sub>2</sub>				0.5	0.4
DOC					
TSM	-0.4	-0.6		0.3	0.6
POC%			0.4	0.6	0.3
POC	-0.4	-0.6		0.5	0.7

**Table 4: Correlations with  $p < 0.05$  (Pearson correlation test) between C or ancillary parameters and the discharge in the different stream orders. The Pearson correlation coefficient is indicated.**

1025

	DOC <sub>budget</sub>	DIC <sub>budget</sub>	POC <sub>budget</sub>
F <sub>GW</sub>	0.2±0.02	6.1±3.0	
F <sub>WL</sub>	1.8±0.6	1.8±1.1	0.4±0.1
F <sub>D</sub>		5.5±2.3	
F <sub>RH</sub>	0.3±0.1	0.3±0.1	
F <sub>OUT</sub>	6.4±3.2	2.2±1.2	0.4±0.1
Imbalance (inputs-outputs)	-4.7	0.5	0

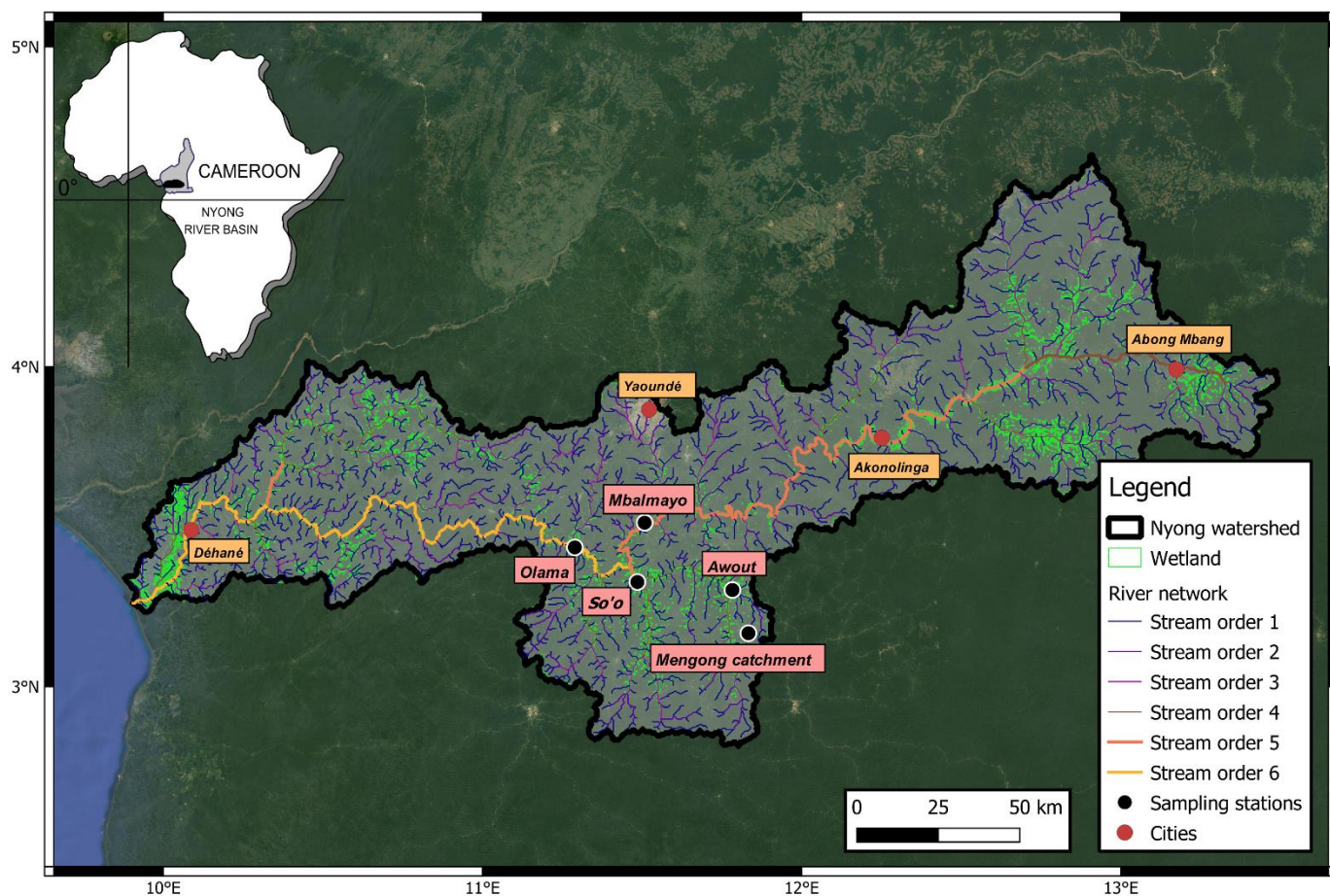
**Table 5: DOC, DIC and POC budgets in the first-order Mengong stream (Eqs. 8-10). Fluxes are in tC yr<sup>-1</sup> and are described in details in the section 2.5. Briefly, F<sub>GW</sub> is the quantity of dissolved carbon leached from non-flooded forest groundwater to the Mengong stream (Eq. 11), F<sub>WL</sub> is the quantity of carbon leached from the Mengong wetland to the Mengong stream (Eqs. 13-14), F<sub>D</sub> is the quantity of C degassed from the Mengong stream to the overlying atmosphere, F<sub>RH</sub> is the heterotrophic respiration in the Mengong stream, and F<sub>OUT</sub> is the quantity of carbon hydrologically exported at the outlet of the Mengong catchment.**

Stream order	$F_{RH}$ mmol m <sup>-2</sup> d <sup>-1</sup>	$k_{600}$ m d <sup>-1</sup>	$F_{degas}$ mmol m <sup>-2</sup> d <sup>-1</sup>	Water surface area km <sup>2</sup>	$F_{degas}$ 10 <sup>3</sup> tC yr <sup>-1</sup>
1	25±11 (46±22 <sup>a</sup> )	2.2±0.1 [2-2.3] 2.6±0.2	1220±640 [560-2760] 1450±570	6.7±3.4 [0.3-11.6] 16.6±7.5	43±26 [14-100] 126±60
2		[2.2-2.8] 2.9±0.3	[670-2450] 1580±610	[2.8-27.2]3 17.1±7.4	[50-220] 137±57
3		[2.5-3.3] 3.0±0.3	[720-2564] 1205±530	[5.7-27.5] 20.2±8.4	[60-240] 114±79
4		[2.5-3.4] 2.3±0.1	[80-2280] 846±350	[8.1-34.1] 23.2±9.4	[4-320] 90±60
5	130±10 (151±31 <sup>a</sup> )	[2.2-2.5] 2.5±0.2	[255-1420] 855±390	[9.6-40.2] 37.0±15.1	[20-220] 141±90
6		[2.3-2.7]	[220-1450]	[15.7-65.1]	[35-320] 650±160 <sup>b</sup> (23.5±5.6 <sup>c</sup> )

1040 **Table 6: At the Nyong watershed scale, yearly averages with standard deviations (based on averaging monthly values in each stream orders) of C degassing rates ( $F_{degas}$  in mmol m<sup>-2</sup> d<sup>-1</sup>),  $k_{600}$ , water surface area, and integrated C degassing flux ( $F_{degas}$  in tC yr<sup>-1</sup>), estimated in the different stream orders. Range (based on monthly values) is shown between brackets. In addition, heterotrophic respiration ( $F_{RH}$ ) measured in the stream orders 1 and 5 is indicated. <sup>a</sup> considering an additional benthic respiration in tropical rivers of 21 mmol m<sup>-2</sup> d<sup>-1</sup> by Cardoso et al. (2014). <sup>b</sup> calculated from the sum of the integrated C degassing flux in each stream order. <sup>c</sup> in tC km<sup>-2</sup> yr<sup>-1</sup>, i.e., the later flux weighed by the surface area of the entire Nyong watershed.**

	$F_{\text{ocean}}$	$F_{\text{degas}}$	$F_{\text{ocean}}$	$F_{\text{degas}}$	Watershed net C sink <sup>a</sup>
	$10^3 \text{ tC yr}^{-1}$	$10^3 \text{ tC-CO}_2 \text{ yr}^{-1}$	$\text{tC km}^{-2} \text{ yr}^{-1}$	$\text{tC-CO}_2 \text{ km}^{-2} \text{ yr}^{-1}$	$\text{tC km}^{-2} \text{ yr}^{-1}$
DOC	130±90		7.2±5.4		
DIC	46±42	650±160	2.5±2.3	23.5±5.6	
POC	12±9		0.6±0.5		
Total	188±100	650±160	10.3±5.8	23.5±5.6	300

1045 **Table 8: At the Nyong watershed scale, averages of monthly hydrological export of C to the ocean ( $F_{\text{ocean}}$ ) and of monthly C degassing to the atmosphere ( $F_{\text{degas}}$ ). <sup>a</sup> the net C sink estimated by Brunet et al. (2009) for the entire Nyong watershed is also indicated.**



1050

**Figure 1: Map of the Nyong watershed showing the river network, the wetland extent from Gumbricht et al., (2017) and the location of the sampling stations and some cities. Note, the Nyong River is displayed bolder than the other rivers. The background map is from Google Satellite®.**



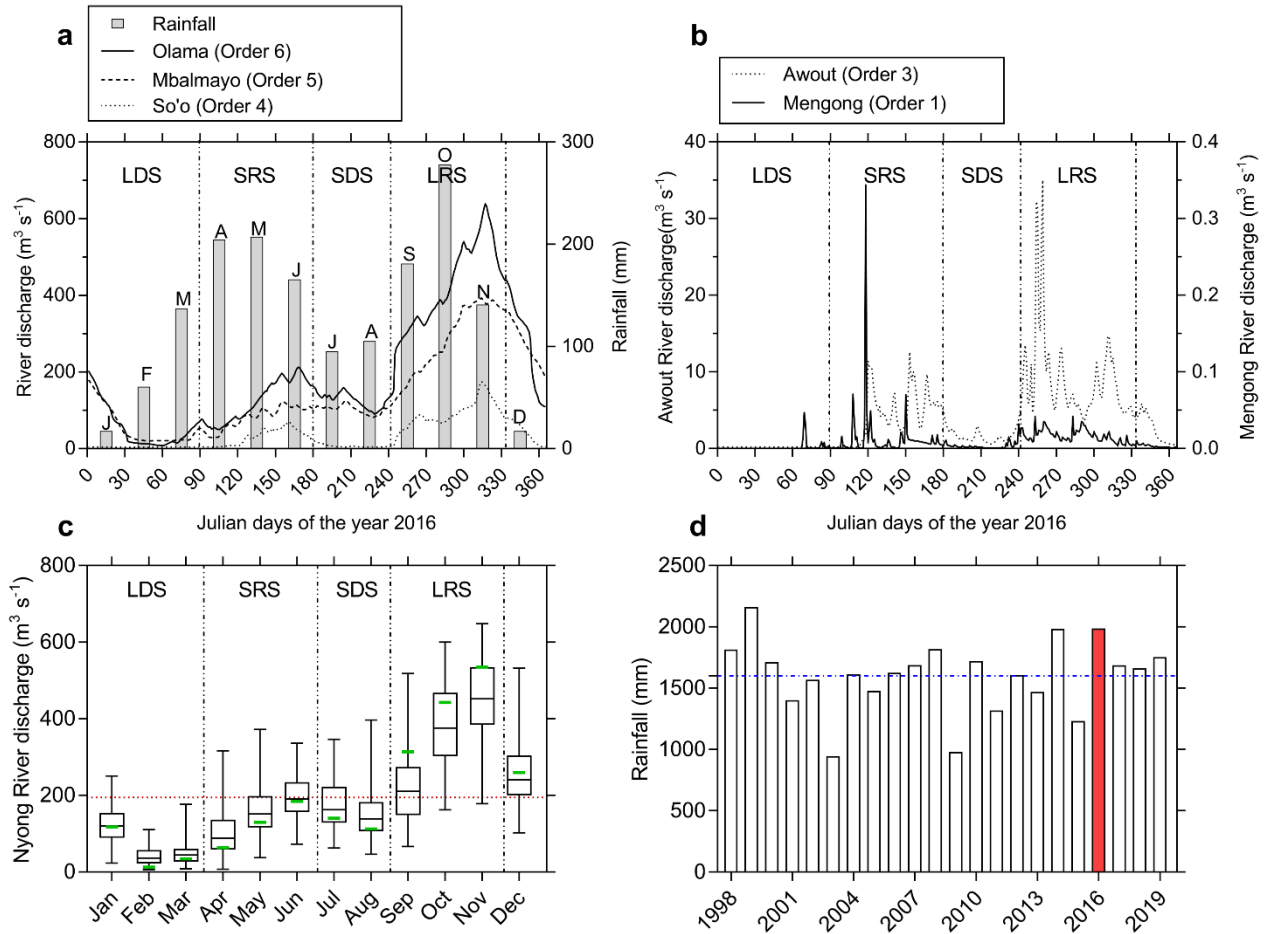


**Figure 2: (a-b) River discharges of the different gauging stations during the sampling year 2016, associated with rainfall measured at the Mengong catchment. (c) The box plots represent the variability of monthly Nyong River discharges from 1998 to 2020 and extreme box plots values represent minimum and maximum monthly discharges during the same period; whereas the green lines represent the average monthly discharges in 2016, and the red dashed line represents the yearly average discharge of  $194.5 \text{ m}^3 \text{s}^{-1}$  for the 1998 to 2020 period (very close to the yearly average discharge of  $195 \text{ m}^3 \text{s}^{-1}$  measured in 2016). (d) Yearly rainfall in the Nyong watershed (measured in the Mengong catchment); the blue line represents the mean rainfall over the 1998-2020 period ( $1600 \pm 290 \text{ mm}$ ), and the red bar represents the yearly rainfall during the sampling year 2016. Hydrologic and rainfall data are from Audry et al. (2021).**

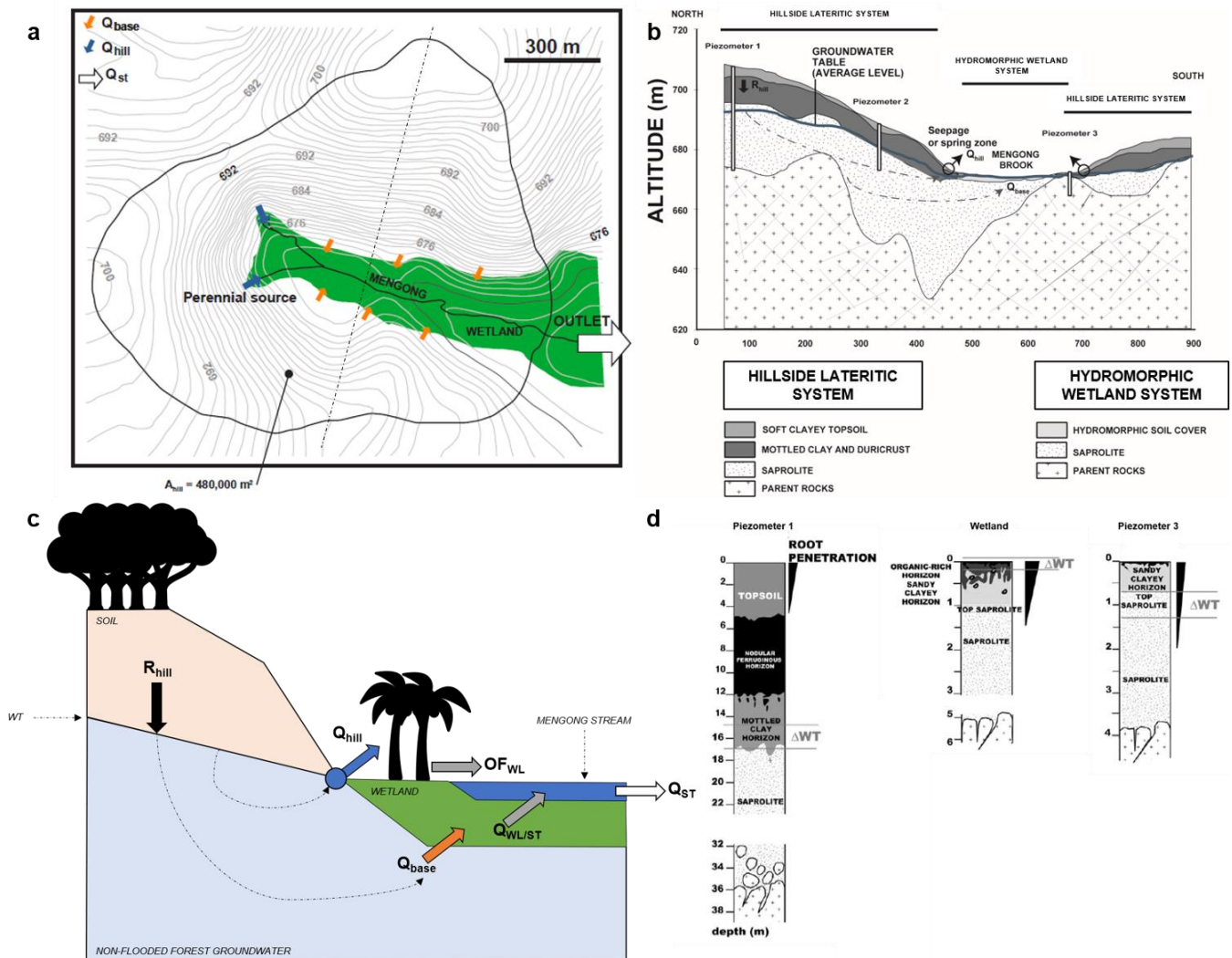
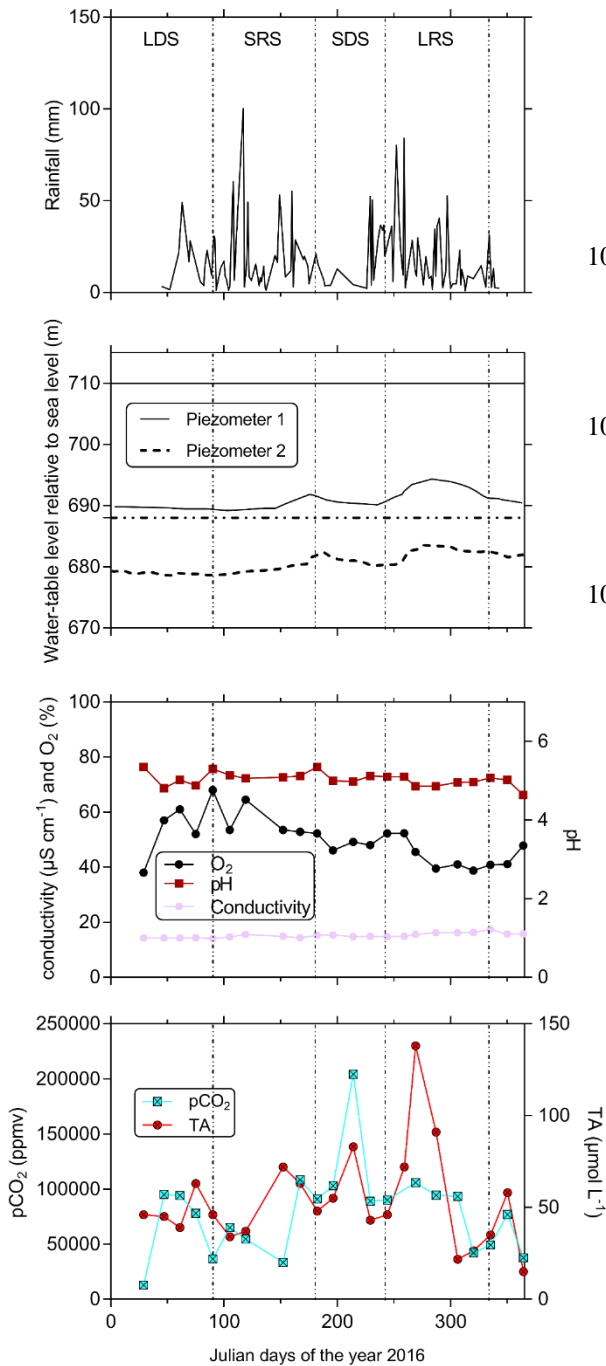
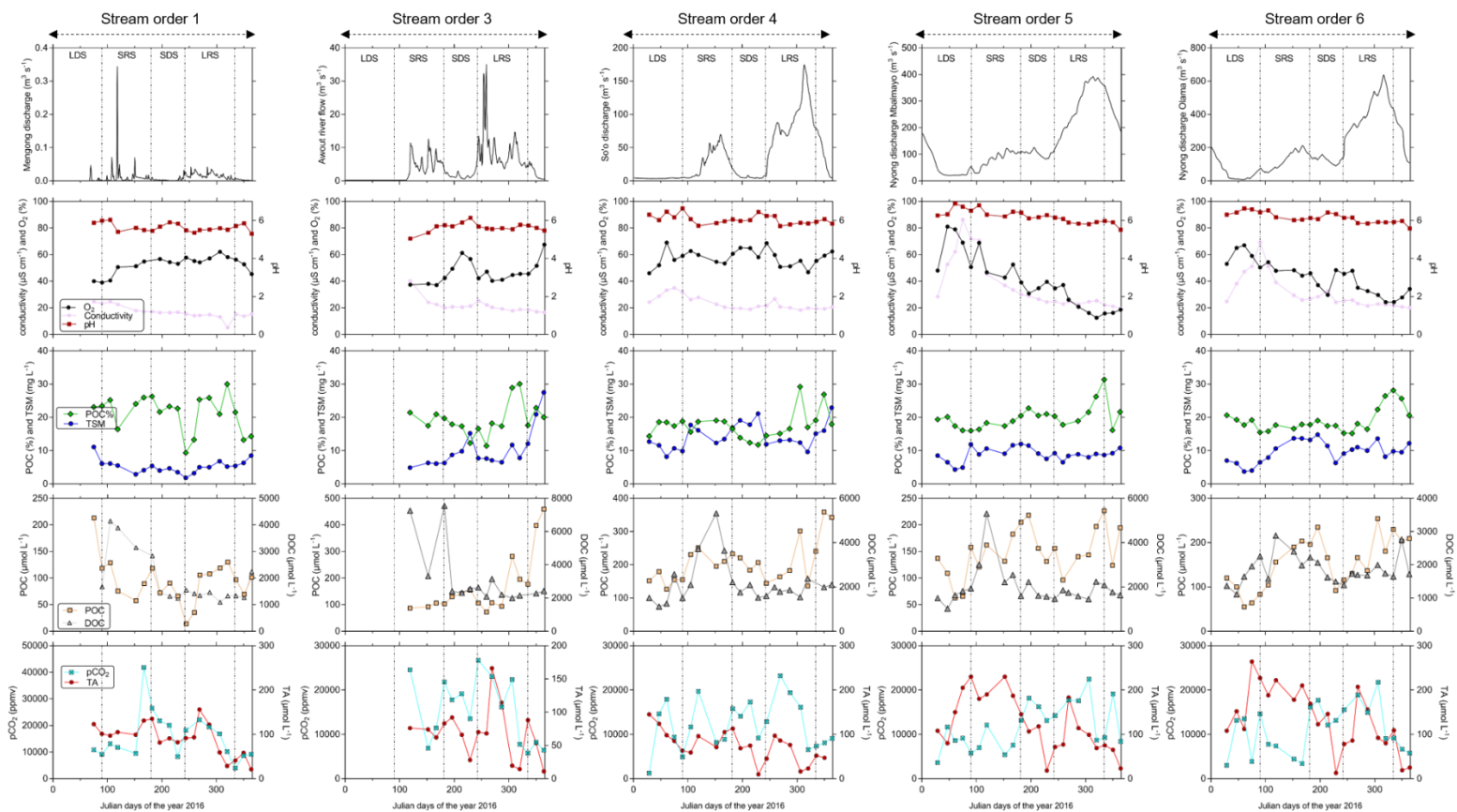


Figure 3: (a) Map of the first-order Mengong catchment showing the wetland area and the hydrological fluxes that are partitioned between the main perennial source ( $Q_{hill}$ , blue arrows) of the non-flooded forest groundwater, specific seepage points all around the hillside/wetland boundaries ( $Q_{base}$ , orange arrows) of the non-flooded forest groundwater, and the discharge at the stream outlet ( $Q_{st}$ , white arrow). Note,  $A_{hill}$  is the surface area drained by the non-flooded forest groundwater. (b) Cross section of the dashed line from the map (a), showing the lithology of the hillside lateritic system and the hydromorphic wetland system, the recharge of the hillside system ( $R_{hill}$ );  $Q_{base}$  and  $Q_{hill}$  are also indicated. (c) Hydrological functioning of the first-order Mengong catchment. Note,  $Q_{WL/ST}$  represents the groundwater flow exchanged between the wetland and the stream and  $OF_{WL}$  is the overland flow on the surface of the wetland. (d) Characteristic soil profiles at piezometers 1, 2 and 3, in which water table level was measured and showed in the Figure 4. Note,  $\Delta WT$  represents the variation of the water table level. The figure 3 was adapted from Braun et al. (2005) and (2012) and from Maréchal et al. (2011).



**Figure 4: temporal variations in the first-order**  
**Mengong catchment of rainfall, water-table level in**  
**piezometer 1 and 2 (see figure 3b) relative to sea**  
**level (elevation of the soil surface at piezometers 1**  
**and 2 relative to sea level is also indicated by the**  
**horizontal lines); and pCO<sub>2</sub>, TA and ancillary**  
**parameters (O<sub>2</sub>, pH, specific conductivity) in non-**  
**flooded forest groundwater (measured at the**  
**perennial source). The temporal variations are**  
**separated into the four seasons that occurs in the**  
**Nyong watershed that are LDS as long dry season,**  
**SRS as short rainy season SDS as short dry season**  
**and LRS as long rainy season.**



1100 **Figure 5: temporal variations of river discharge, carbon (pCO<sub>2</sub>, TA, DOC, POC) and ancillary parameters (O<sub>2</sub>, pH, specific conductivity, TSM) in surface waters of the Nyong watershed. The temporal variations are separated into the four seasons that occurs in the Nyong watershed that are LDS as long dry season, SRS as short rainy season SDS as short dry season and LRS as long rainy season.**

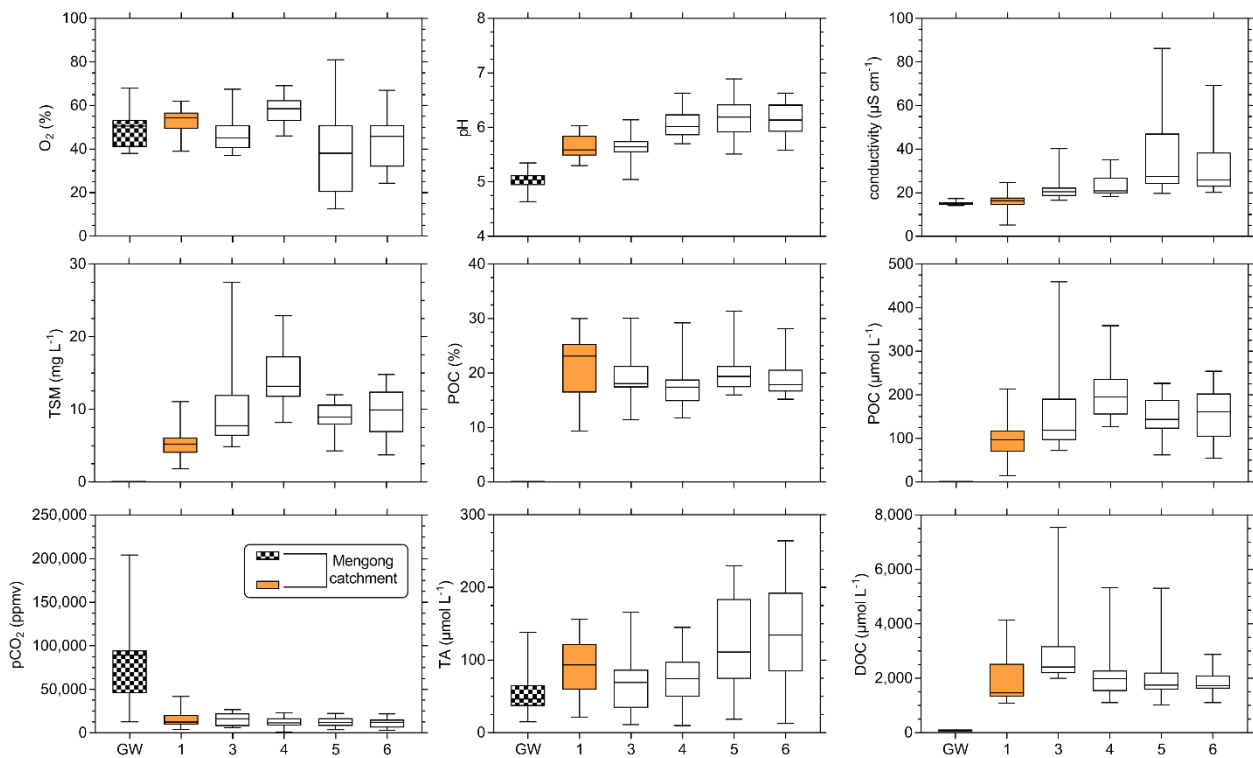


**Figure 6: spatial variations of carbon parameters (pCO<sub>2</sub>, TA, DOC, POC) and ancillary parameters (O<sub>2</sub>, pH, specific conductivity, TSM) across non-flooded forest groundwater (GW) and streams orders 1, 3, 4, 5 and 6 in the Nyong watershed.**

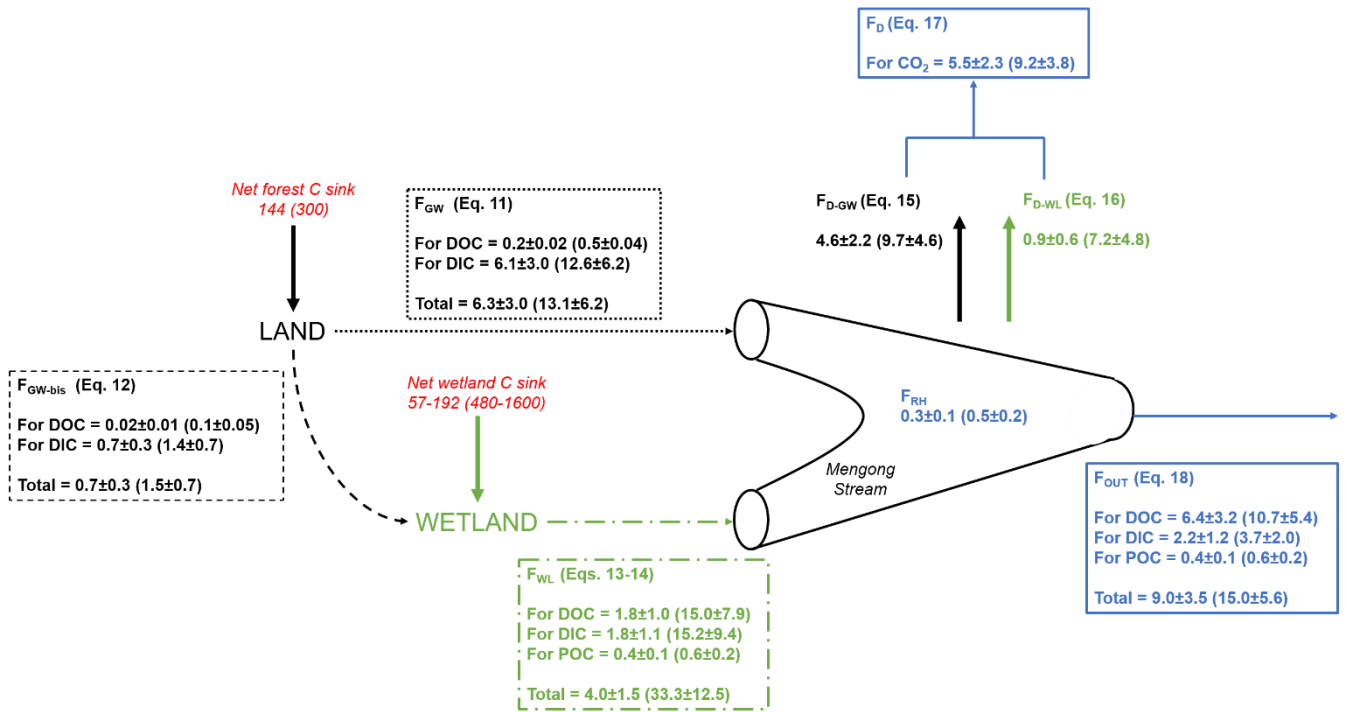
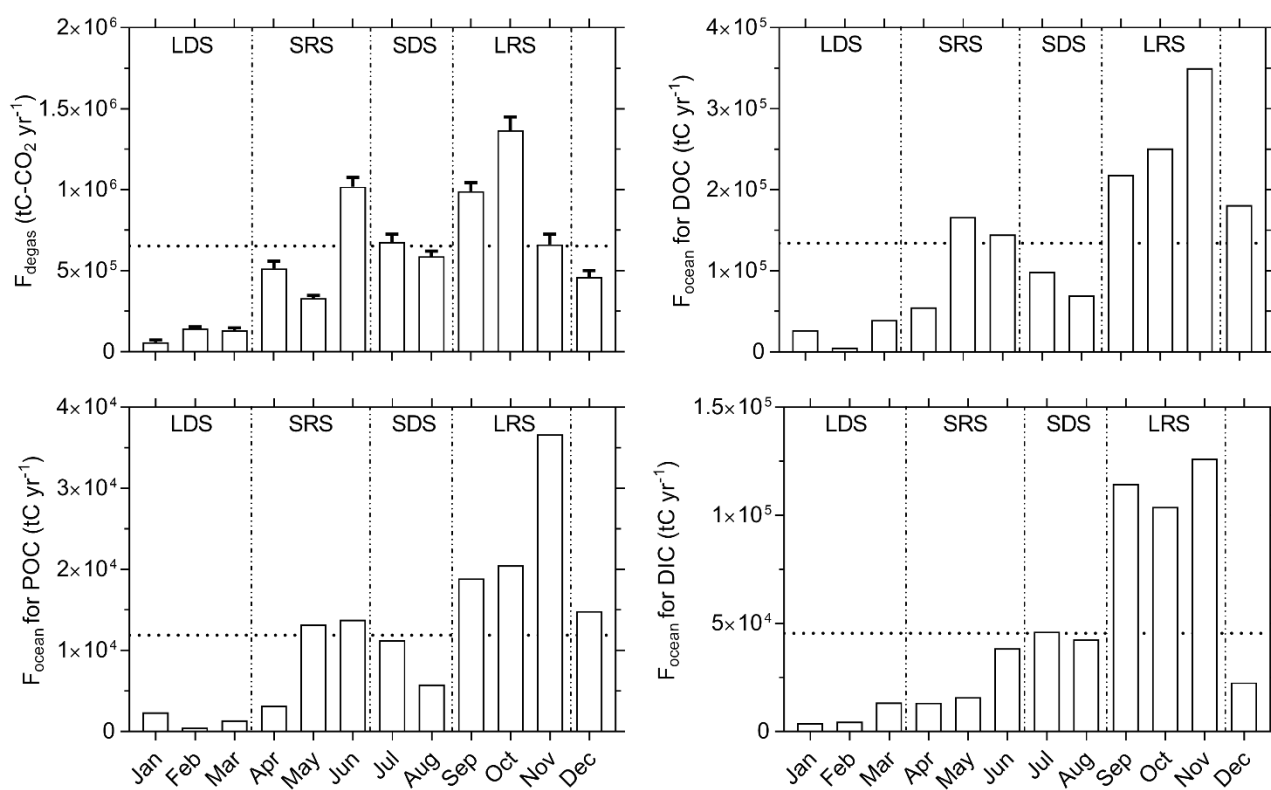
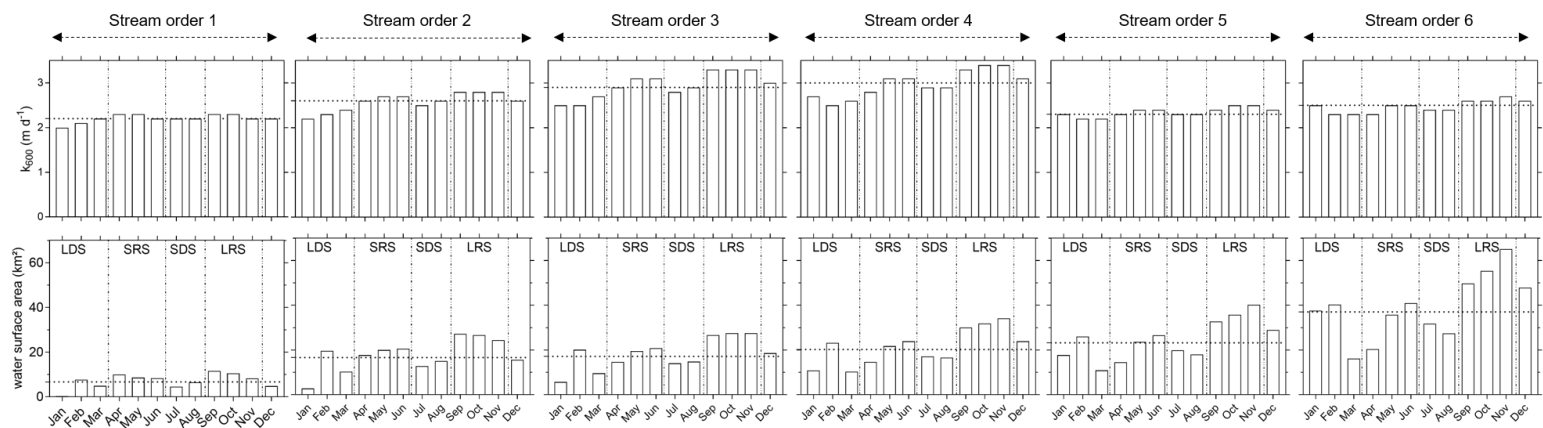


Figure 7: mass balance of C in the first order Mengong catchment. All fluxes are in tC yr<sup>-1</sup>, and in tC km<sup>-2</sup> yr<sup>-1</sup> when between brackets (weighed by the surface area of 0.48 km<sup>2</sup> drained by non-flooded forest groundwater for the net forest C sink, F<sub>GW</sub>, F<sub>GW-bis</sub> and F<sub>D-GW</sub>, by the wetland surface area of 0.12 km<sup>2</sup> for the net wetland C sink, F<sub>WT</sub> and F<sub>D-W</sub>, and by the Mengong catchment area of 0.6 km<sup>2</sup> for F<sub>OUT</sub>, F<sub>D</sub> and F<sub>RH</sub>), and they are associated with their corresponding equations as described in details in the section 2.5. Briefly, F<sub>GW</sub> is the quantity of dissolved carbon leached from non-flooded forest groundwater to the Mengong stream (Eq. 11), F<sub>GW-bis</sub> is the quantity of dissolved carbon leached from non-flooded forest groundwater to the Mengong wetland (Eq. 12), F<sub>WL</sub> is the quantity of carbon leached from the Mengong wetland to the Mengong stream (Eqs. 13-14), F<sub>D</sub> is the quantity of C degassed from the Mengong stream to the overlying atmosphere, F<sub>RH</sub> is the heterotrophic respiration in the Mengong stream, and F<sub>OUT</sub> is quantity of carbon hydrologically exported at the outlet of the Mengong catchment. In addition, net local forest C sink of mature forest of the Mengong catchment estimated by Brunet et al. (2009), and a range of typical net wetland C sink measured in wetlands in Africa by Saunders et al. (2007) and Jones and Humphries (2002) are both indicated.



**Figure 8: Monthly C fluxes at the Nyong watershed scale described in the section 2.4. The dashed lines represent the yearly average of the different monthly C fluxes. The figures are separated into the four seasons that occurs in the Nyong watershed that are LDS as long dry season, SRS as short rainy season SDS as short dry season and LRS as long rainy season.**



1135 **Figure S1: Monthly variations of  $k_{600}$  (m d<sup>-1</sup>) and water surface area (km<sup>2</sup>) in each stream order across seasons. The temporal variations are separated into the four seasons that occurs in the Nyong watershed that are LDS as long dry season, SRS as short rainy season SDS as short dry season and LRS as long rainy season.**